

UNCLASSIFIED

AD NUMBER

AD842559

LIMITATION CHANGES

TO:

Approved for public release; distribution is unlimited. Document partially illegible.

FROM:

Distribution authorized to U.S. Gov't. agencies and their contractors; Critical Technology; SEP 1968. Other requests shall be referred to Air Force Technical Application Center, Washington, DC. Document partially illegible. This document contains export-controlled technical data.

AUTHORITY

usaf ltr, 25 jan 1972

THIS PAGE IS UNCLASSIFIED

AD 842559

# BODY WAVE MAGNITUDE AND SOURCE MECHANISM

30 September 1968

Prepared For

AIR FORCE TECHNICAL APPLICATIONS CENTER  
Washington, D. C.

By

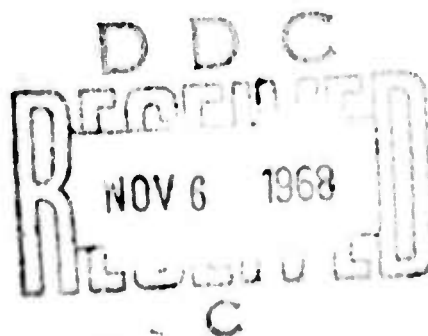
H. S. Jarosch  
TELEDYNE, INC.

Under

Project VELA UNIFORM

Sponsored By

ADVANCED RESEARCH PROJECTS AGENCY  
Nuclear Test Detection Office  
ARPA Order No. 624



# DISCLAIMER NOTICE

THIS DOCUMENT IS THE BEST  
QUALITY AVAILABLE.

COPY FURNISHED CONTAINED  
A SIGNIFICANT NUMBER OF  
PAGES WHICH DO NOT  
REPRODUCE LEGIBLY.

BODY WAVE MAGNITUDE AND SOURCE MECHANISM  
SEISMIC DATA LABORATORY REPORT NO. 225

AFTAC Project No.:	VELA T/6702
Project Title:	Seismic Data Laboratory
ARPA Order No.:	624
ARPA Program Code No.:	8F10
Name of Contractor:	TELEDYNE INDUSTRIES, INC.
Contract No.:	F 33657-68-C-0945
Date of Contract:	2 March 1968
Amount of Contract:	\$ 1,251,000
Contract Expiration Date:	1 March 1969
Project Manager:	Royal A. Hartenberger (703) 836-7647

P. O. Box 334, Alexandria, Virginia

AVAILABILITY

This document is subject to special export controls and each transmittal to foreign governments or foreign nationals may be made only with prior approval of Chief, AFTAC.

*attn: VSC, Wash D.C. 20333*

This research was supported by the Advanced Research Projects Agency, Nuclear Test Detection Office, under Project VELA-UNIFORM and accomplished under technical direction of the Air Force Technical Applications Center under Contract F 33657-68-C-0945.

Neither the Advanced Research Projects Agency nor the Air Force Technical Applications Center will be responsible for information contained herein which may have been supplied by other organizations or contractors, and this document is subject to later revision as may be necessary.

# ABSTRACT

A new method is proposed for improving the body-wave magnitude determination by using the observed values of the body-wave magnitude ( $m_b$ ) together with the first motion directions, to obtain by least squares analysis the best double couple source parameters; the resulting radiation pattern is then integrated spatially to provide a corrected estimate of the magnitude. Results for a number of events previously studied by other investigators are presented.

## TABLE OF CONTENTS

	Page No.
ABSTRACT	
INTRODUCTION	1
METHOD	4
Algorithm for Obtaining Source Parameters	8
AMBIGUITY OF RESULTS	9
Second Solution of the Fault Plane	9
ESTABLISHING THE METHOD	14
INPUT DATA	15
Analysis of the Data	15
CONCLUSIONS	19
Suggestions for Future Research	19
ACKNOWLEDGEMENTS	21
REFERENCES	22
APPENDIX	

## LIST OF TABLES

Table Title	Table No.
Fault Plane Solutions Using the New Method	1
Fault Plane Solutions Previously Obtained	2
Example of Input Data for the Banda Sea Earthquake of 21 March 1964.	3
Results for the Banda Sea Earthquake of 21 March 1964.	4
Results for the Rat Island Earthquake of 5 February 1964.	5
Results for the Rat Island Earthquake of 1 October 1965.	6
Results for the Rat Island Earthquake of 15 May 1966.	7
Results for the Rat Island Earthquake of 4 July 1966.	8
Results for the Rat Island Earthquake of 22 November 1965.	9
Results for the Rat Island Earthquake of 22 November 1965 (additional magnitudes).	10
Results for the Hindu Kush Earthquake of 28 January 1964.	11
Results for the Alaskan Earthquake of 28 March 1964.	12
Results for the Alaskan Earthquake of 28 March 1964 (additional first motions).	13
Results for the Niigata Earthquake of 16 June 1964.	14



## LIST OF FIGURES

Figure Title	Figure No.
Observed Radiation Pattern for the Banda Sea Earthquake of 21 March 1964.	1
Calculated Radiation Pattern for the Banda Sea Earthquake of 21 March 1964.	2
Observed Radiation Pattern for the Rat Island Earthquake of 5 February 1965.	3
Calculated Radiation Pattern for the Rat Island Earthquake of 5 February 1965.	4
Observed Radiation Pattern for the Rat Island Earthquake of 1 October 1965.	5
Calculated Radiation Pattern for the Rat Island Earthquake of 1 October 1965.	6
Observed Radiation Pattern for the Rat Island Earthquake of 15 May 1966.	7
Calculated Radiation Pattern for the Rat Island Earthquake of 15 May 1966.	8
Observed Radiation Pattern for the Rat Island Earthquake of 4 July 1966.	9
Calculated Radiation Pattern for the Rat Island Earthquake of 4 July 1966.	10
Observed Radiation Pattern for the Rat Island Earthquake of 22 November 1965.	11
Calculated Radiation Pattern for the Rat Island Earthquake of 22 November 1965.	12
Observed Radiation Pattern for the Rat Island Earthquake of 22 November 1965 (additional magnitudes).	13
Calculated Radiation Pattern for the Rat Island Earthquake of 22 November 1965 (additional magnitudes).	14
Observed Radiation Pattern for the Hindu Kush Earthquake of 28 January 1964.	15

# LIST OF FIGURES (CONT'D.)

Figure Title	Figure No.
Calculated Radiation Pattern for the Hindu Kush Earthquake of 28 January 1964.	16
Observed Radiation Pattern for the Alaskan Earthquake of 28 March 1964.	17
Calculated Radiation Pattern for the Alaskan Earthquake of 28 March 1964.	18
Calculated Radiation Pattern for the Alaskan Earthquake of March 28, 1964 (additional first motions).	19
Observed Radiation Pattern for the Niigata Earthquake of 16 June 1964.	20
Calculated Radiation Pattern for the Niigata Earthquake of 16 June 1964.	21
Geometry of a Shear Dislocation Source.	22

## INTRODUCTION

The body-wave magnitude of an earthquake was defined by Gutenberg and Richter as

$$m_b = \log_{10} A/T + Q - 3$$

where

A is the P-wave amplitude in millimicrons

T is the period in seconds

Q is the Gutenberg-Richter (1956) distance-depth correction.

This magnitude of course, depends on the amplitude recorded at a particular station observing the earthquake. For want of a better method, the arithmetic mean of individual station magnitudes was chosen to be representative of the true body-wave magnitude. This would be correct if the source were assumed to be purely compressional (azimuthally uniform).

However, our knowledge of source mechanisms has increased to a point where it is now known that the mechanism of most earthquakes may be well represented by a double couple source mechanism, Stauder and Bollinger (1964). This, in turn, implies that the body-wave radiation pattern is not azimuthally uniform. If we want to be still more accurate, we can also include the effect of a moving source. In any case, the arithmetic mean of the observations does not represent the mean of a radiation pattern caused by a fixed or moving double couple. Hence it is desirable to find a better way of defining the "true" body-wave magnitude.

We propose that a better measure of the "true" body-wave magnitude may be obtained by taking the amplitude of a purely compressional source whose radiation pattern has the same area as the observed radiation pattern.

Naturally, this means that we have to know the source parameters, i.e., the dip direction, dip angle and slip angle of the fault plane and the auxiliary plane.

In order to find the source parameters, two totally different methods have been used to date. The first is a purely geometrical approach, using only the directions of the first motion of P-waves. More recently the study of the polarization angle of the S-wave has further helped to improve estimation of the source parameters. However, as Stauder and Nuttli (1965) point out:

"Examination of multiple solutions, i.e., by several different authors for one and the same earthquake, as also a comparison of groups of fault plane solutions for a given region evidence poor agreement and systematic differences in solutions by different authors. This evidence requires that caution should be exercised in drawing conclusions from the existing accumulation of published fault plane solutions."

Although some of the directions of the first motions of the P-waves are reported, no data are readily available on polarization angles, and hence a detailed visual study of the seismograms is necessary for the analysis of source parameters using the above method.

The second method which has been used is spectral equalization. This is applicable to both body and surface waves and source parameters may be obtained, but with this method it is necessary to use digitized seismograms of a worldwide network, which are not readily available.

The method which we propose here consists of using data which are readily available, i.e., reported first motion directions together with observed body-wave magnitudes as given by the C&GS Earthquake Data Reports and the ISC Bulletin.



Of course, the method is bound to be inaccurate if there are large gaps in the azimuthal coverage, but in this case the other methods also fail. It is hoped that for earthquakes of magnitude 5 and larger, an approximate solution of the source parameters may be obtained and hence a better value of the mean body-wave magnitude may be established.

## METHOD

The method is based on a number of assumptions:

1. Using only WWNSS stations, it is not necessary to make instrumental corrections since the  $m_b$  is computed on the basis of A/T and the instrument responses are nearly identical.
2. Geometrical spreading is accounted for by the Gutenberg-Richter correction for distance and depth of focus.
3. The major contribution to the difference in the observed variation of  $m_b$  with azimuth is caused by the source radiation pattern.
4. A double-couple source accounts for the radiation pattern.
5. Sufficient azimuthal coverage exists in the observations to allow reasonably unambiguous determination of the source mechanism.

This method is not intended to replace the body-wave equalization procedure as given by Ben Menahem, et al (1965). It is intended to provide a small correction to the mean  $m_b$ .

The model taken is the linear regression with zero intercept

$$B_i = KA_i + e_i$$

where  $B_i$  is the observed amplitude ( $B_i = 10^{M_i}$ )  
 $K$  is a constant to be determined  
 $A_i$  is the calculated amplitude (as given by Ben Menahem et al (1965))  
 $e$  is the error in the  $i$ th observation.

The calculated amplitude at the  $i$ 'th station is related to the source parameters by:

$$A_i = a_0 + a_1 \sin(\theta - \theta_0) + a_2 \sin 2(\theta - \theta_0) + b_1 \cos(\theta - \theta_0) + b_2 \cos 2(\theta - \theta_0)$$

where

$$a_0 = 1/4 \sin \lambda \sin 2\delta (3 \cos^2 i_h - 1)$$

$$a_1 = 1/2 \sin \lambda \cos 2\delta \sin 2i_h$$

$$b_1 = 1/2 \cos \lambda \cos \delta \sin 2i_h$$

$$a_2 = -1/2 \cos \lambda \sin \delta \sin 2i_h$$

$$b_2 = 1/4 \sin \lambda \sin 2\delta \sin 2i_h$$

$\theta$  is the azimuth (east of north) of the station as seen from the epicenter

$\theta_0$  is the azimuth (east of north) of the strike direction of the assumed fault plane.

$\delta$  is the dip angle

$\lambda$  is the slip angle

$i_h$  is the take-off angle

Figure 22 shows the geometry of the source parameters.

We wish to use a least squares procedure to determine the source parameters. To do this, we minimize the sum of the squares of the errors, i.e., we choose  $\hat{K}$  so that

$$E = \sum e_i^2 = \sum (B_i - KA_i)^2 \text{ is minimized.}$$

Hence the estimated value for  $K$  is given by

$$\hat{K} = \frac{\sum B_i A_i}{\sum A_i^2}$$

Since  $A_i(\lambda) = -A_i(\lambda+180^\circ)$  we determine which half-plane has the smaller error, by choosing

$$\hat{K} = \frac{|\sum B_i A_i|}{\sum A_i^2}$$

$$\text{and then } e_i = \begin{cases} B_i - \hat{K}A_i & \text{for } 0^\circ \leq \lambda < 180^\circ \\ B_i + \hat{K}A_i & 180^\circ \leq \lambda < 360^\circ \end{cases}$$

Only stations for which we have values of  $m_b$  were used in the estimation of  $\hat{K}$ . In order to include also stations for which  $m_b$  is not given, but the first motion direction is given, we assumed an observed value whose absolute value was that of the calculated value and whose sign was the sign of the observed first motion, i.e.,

$$B_i = \text{sign}(STA_i) \hat{K}|A_i|$$

so that the contribution  $e_i = 0$  if the signs of the observed and calculated values were the same and  $2\hat{K}|A_i|$  if the signs were opposite. This helps to insure that the sign of the larger amplitudes will cause a larger error, if they are different from the observed.

In order to calculate the mean  $m_b$ , it is first necessary to define a mean amplitude for a radiation pattern. We intend to use as a mean amplitude the amplitude of a purely compressional (azimuthally uniform) source whose radiation pattern has the same area as the observed radiation pattern:

$$\pi \bar{A}_i^2 = 1/2 \int_0^{2\pi} A_i^2(\theta) d\theta.$$



This leads to

$$\bar{A}_i = \left\{ \frac{1}{\pi} [a_0^2 + 1/2 (a_1^2 + a_2^2 + b_1^2 + b_2^2)] \right\}^{1/2}$$

Now since the coefficients  $a_0$ ,  $a_1$ ,  $a_2$ ,  $b_1$  and  $b_2$  are functions of the take-off angle  $i_h$  (which is different for each station), we simply compute an arithmetic mean of the means  $\bar{A}_i$ , so that finally the mean amplitude is given by

$$\bar{A} = \frac{\hat{K}}{N} \sum_{i=1}^N \bar{A}_i$$

and hence the mean  $m_b$  is given by

$$\bar{M} = \log_{10} \bar{A}.$$

We have thus calculated a new mean value of  $m_b$  which has been corrected for the radiation pattern. The standard error of estimation of the corrected  $m_b$  can be calculated from the t-distribution. Arbitrarily taking our confidence limits at 90%, we find

$$\hat{K}_+ = \hat{K} + \frac{t_{.95}^{N-1} S}{\left( \sum_{i=1}^N A_i^2 \right)^{1/2}}$$

$$\hat{K}_- = \hat{K} - \frac{t_{.95}^{N-1} S}{\left( \sum_{i=1}^N A_i^2 \right)^{1/2}}$$

where  $S^2 =$

$$\frac{1}{N-1} \sum_{i=1}^N (B_i - \hat{K}A_i)^2 = \frac{1}{N-1} \sum_{i=1}^N \hat{\ell}_i^2$$

$t_{.95}^{N-1}$  is the value of the student's t-distribution at the 95% confidence limit, for  $n-1$  degrees of freedom.

Hence the upper and lower confidence limit for the body wave magnitude is found from

$$\bar{M}_+ = \log_{10} \bar{A}_+$$

$$\bar{M}_- = \log_{10} \bar{A}_-$$

$$\text{where } \bar{A}_+ = \frac{\hat{K}_+}{N} \sum_{i=1}^N \bar{A}_i$$

$$\bar{A}_- = \frac{\hat{K}_-}{N} \sum_{i=1}^N \bar{A}_i$$

These values are shown in Table 1.

#### Algorithm for Obtaining Source Parameters

The initial strike angle, step size and number of steps are given as input parameters. A coarse mesh search is carried out to find the best strike angle and dip and slip angles. The step size for the dip and slip angles is taken to be  $10^\circ$ .

A fine mesh search is then carried out keeping the strike angle found in the first stage fixed and varying the dip and slip angles to find the least squares fit, in steps of  $1^\circ$ . Details are given in the flow chart in the appendix to this report.

## AMBIGUITY OF RESULTS

When one finds a fault-plane solution using first motions only, there exists an ambiguity in the result, in that it is not possible to decide which is the fault plane and which is the auxiliary plane. Similarly, using the radiation pattern, Ben Menahem et al., (1965) found the amplitudes and directions of compressional, SV and SH radiation to be:

$$\vec{U}_P = \left\{ \frac{L_0 ds}{2\pi v_P} \left( \frac{v_s}{v_P} \right)^2 \right\} (\vec{a} \cdot \vec{R}) (\vec{n} \cdot \vec{R}) \vec{R}$$

$$\vec{U}_{SV} = \left\{ \frac{L_0 ds}{4\pi v_s} \right\} \left[ (\vec{n} \cdot \vec{R}) (\vec{a} \cdot \vec{\theta}) + (\vec{a} \cdot \vec{R}) (\vec{n} \cdot \vec{\theta}) \right] \vec{\theta}$$

$$\vec{U}_{SH} = \left\{ \frac{L_0 ds}{4\pi v_s} \right\} \left[ (\vec{n} \cdot \vec{R}) (\vec{a} \cdot \vec{\theta}) + (\vec{a} \cdot \vec{R}) (\vec{n} \cdot \vec{\theta}) \right] \vec{\theta}$$

where

$\vec{a}$  is the vector in the direction of motion

$\vec{n}$  is the vector normal to the fault plane.

Since the vector  $\vec{a}$ , the direction of motion, is normal to the auxiliary plane and  $\vec{n}$  is the vector normal to the fault plane, it can be seen that the radiation pattern is unchanged by the interchange of  $\vec{a}$  and  $\vec{n}$ ; thus the same ambiguity which exists for the fault-plane solution, also exists for the radiation pattern method.

### Second Solution of the Fault Plane

In the previous section we explained that in finding a solution of the source parameters, there exists another solution, whose radiation pattern is identical with that

already found. Hence, since we do not know which is the fault plane and which is the auxiliary plane, it is necessary to compute also the second solution. By comparing the mechanisms of groups of earthquakes from the same area having similar depth of focus, we might be able to see that one of the planes is similar in all cases in order to decide that this is the fault plane, assuming that the source mechanism does not change greatly.

It is assumed that one solution of  $\theta_0$ ,  $\delta$  and  $\lambda$  has been found already. In Ben Menahem et al (1965) the three coordinate axes are taken in the strike direction ( $x_1$ ), a direction opposite to the horizontal projection of the dip direction ( $x_2$ ) and vertically upwards ( $x_3$ ).

Making a transformation so that we have  $x'_1$  pointing North,  $x'_2$  West and  $x'_3$  vertically upwards for a righthand system, we can describe the transformation of the unit vectors by the matrix relation:

$$\begin{bmatrix} \vec{e}_1 \\ \vec{e}_2 \\ \vec{e}_3 \end{bmatrix} = \begin{bmatrix} \cos \theta_0 & \sin \theta_0 & 0 \\ -\sin \theta_0 & \cos \theta_0 & 0 \\ 0 & 0 & 1 \end{bmatrix} \begin{bmatrix} \vec{e}'_1 \\ \vec{e}'_2 \\ \vec{e}'_3 \end{bmatrix}$$

where  $\theta_0$  is the strike angle measured clockwise from North.

Hence we can describe the direction of motion, the "null" vector and the vector perpendicular to the direction of motion

by the matrix relation

$$\begin{array}{rcl}
 \vec{a} & \begin{array}{l} \cos \lambda \cos \theta_0 - \sin \lambda \cos \delta \sin \theta_0 \\ \sin \lambda \cos \theta_0 - \cos \lambda \cos \delta \sin \theta_0 \\ \sin \delta \sin \theta_0 \end{array} & \begin{array}{l} \cos \lambda \sin \theta_0 + \sin \lambda \cos \delta \cos \theta_0 \\ \sin \lambda \sin \theta_0 + \cos \lambda \cos \delta \cos \theta_0 \\ -\sin \delta \cos \theta_0 \end{array} \begin{array}{l} \sin \lambda \sin \delta \\ \cos \lambda \sin \delta \\ \cos \delta \end{array} \begin{array}{l} \vec{e}_1 \\ \vec{e}_2 \\ \vec{e}_3 \end{array} \\
 \vec{b} & = & \\
 \vec{n} & & 
 \end{array} \quad (2)$$

The vector  $\vec{a}$  lies in the fault plane in the direction of motion and hence its direction cosines are the direction cosines of the auxiliary plane, which is normal to the fault plane. The vector  $\vec{n}$  is normal to the fault plane and hence its direction cosines are the direction cosines of the fault plane. The vector  $\vec{b}$  lies in the fault plane normal to the direction of motion and hence it is the "null" vector, the intersection of the fault

plane and the auxiliary plane.

These relations are needed to compute the slip angles, assuming that each plane in turn represents the fault plane.

Given one solution of the source parameters  $\theta_1, \delta_1, \lambda_1$  we wish to find the second solution  $\theta_2, \delta_2, \lambda_2$ . We can do this by remembering that  $\vec{a}_1$  and  $\vec{n}_1$  of one solution become  $\vec{n}_2$  and  $\vec{a}_2$  of the other solution and hence by equating direction cosines, we have

$$\cos \lambda_1 \cos \theta_1 + \sin \lambda_1 \cos \delta_1 \sin \theta_1 = - \sin \delta_2 \sin \theta_2 \quad (3)$$

$$\cos \lambda_1 \sin \theta_1 - \sin \lambda_1 \cos \delta_1 \cos \theta_1 = \sin \delta_2 \cos \theta_2 \quad (4)$$

$$- \sin \lambda_1 \sin \delta_1 = - \cos \delta_2 \quad (5)$$

From these we can derive the expression for the constraint of perpendicularity between the two planes

$$\tan \delta_1 \tan \delta_2 \cos (\theta_1 - \theta_2) = - 1 \quad (6)$$

and the reciprocal relations

$$\cos \delta_1 = \sin \lambda_2 \sin \delta_2 \quad (7)$$

$$\cos \delta_2 = \sin \lambda_1 \sin \delta_1 \quad (8)$$

$$\cos \lambda_1 = \sin \delta_2 \sin (\theta_2 - \theta_1) \quad (9)$$

$$\cos \lambda_2 = \sin \delta_1 \sin (\theta_1 - \theta_2) \quad (10)$$



Hence, having found one solution for  $\theta_1$ ,  $\delta_1$ ,  $\lambda_1$ , we find  $\theta_2$ ,  $\delta_2$ ,  $\lambda_2$  by finding  $\delta_2$  from equation (8) where  $\delta_2$  is defined to be between  $0^\circ$  and  $180^\circ$ . In order to find  $\lambda_2$  we use equations (7), (9), and (10) and then we can fit  $\lambda_2$  into the correct quadrant. Finally, we compute  $\theta_2$  by using equations (6) and (9) and thus we can fit  $\theta_2$  into the correct quadrant. When,  $90^\circ < \delta_2 \leq 180^\circ$ , it signifies that the dip direction lags  $90^\circ$  behind the strike direction, instead of leading by  $90^\circ$ , according to the sign convention used here.

## ESTABLISHING THE METHOD

In order to show that the method yields significant results, the following test cases were tried:

1. Banda Sea Earthquake of March 21, 1964 (reported by Teng and Ben Menahem (1965). For this case the calculated amplitudes were also input to check that the method gives back the exact input values.

2. Rat Island Earthquake of 5 February 1965 (origin time 09 32 9.3). The Rat Island earthquake mechanisms were reported by Stauder (1968). The information for the first motion directions for the Rat Island sequence was kindly supplied by the Rev. William Stauder, S.J. in a private communication.

3. Rat Island Earthquake of 1 October 1965

4. Rat Island Earthquake of 15 May 1966.

5. Rat Island Earthquake of 4 July 1966.

6. Rat Island Earthquake of 22 November 1965.

7. Hindu-Kush Earthquake of 28 January 1964. Fault plane solutions were reported by Hedayati and Hirasawa (1966), and also by Ritsema (1966).

8. Alaskan Earthquake of 28 March 1964 (origin time 03 36 14.2). The input data was taken from the Bulletin of the International Seismological Centre. Solutions were reported by Stauder et al (1966), and Harding et al (1968).

9. Niigata Earthquake of 16 June, 1964. A fault plane solution was reported by Hirasawa (1965).



## INPUT DATA

Input data were collected mainly from the C & GS Earthquake Data Reports and the Bulletin of the International Seismological Center, Edinburgh.

The first motion data for the Banda Sea earthquake were taken from Teng and Ben Menahem (1965).

The first motion data for the Rat Island earthquakes were supplied by the Rev. William Stauder, S.J., in a private communication.

The first motion data for the Hindu-Kush earthquake were taken from Hedayati and Hirasawa (1966).

The additional first motion data for the Alaskan earthquake were supplied by Harding in a preprint.

The first motion data for the Niigata earthquake were taken from Hirasawa (1965).

### Analysis of the Data

1. Banda Sea Earthquake of the 21st of March 1964. For this earthquake 37 stations were used, 12 of them with magnitude and 25 with only first motions. Figure 1 shows the observed radiation pattern and Table 3 shows the input data. Figure 2 shows the calculated radiation pattern and Table 4 gives the results in tabular form. In our final solution, 36 stations had the same calculated and observed first motion direction and the one disagreement was near a nodal value. The new mean value of  $m_b$  came out to be 5.85 as against the C&GS value of 5.8. The stars in Figure 2 are calculated amplitudes for those stations which had observed values and the dots are calculated amplitudes for those stations which only reported first motion directions.

2. Rat Island Earthquake of the 5th of February 1965 (9h.) Figure 3 shows the observed radiation pattern. For this case 72 stations were used, 13 of them with magnitude and 59 with first motions only. The results are given in Figure 4 and Table 5. The resulting score was 72-12, i.e., 12 stations had the opposite calculated first motion. However, this earthquake showed clearly that the C&GS value of  $m_b$  was too low since most of the observations were near nodes. The new value of  $m_b$  was 6.3 as against the C&GS value of 5.9.

3. Rat Island Earthquake of the 1st of October 1965. This was a case where all the observed first motion consisted of dilatations. Figure 5 shows the observed radiation pattern. The results are given in Figure 6 and Table 6. The score was 80-0. Although the strike angle is quite far from that found by Stauder (1968), the pattern of signs of the first motion are completely similar to Stauder's and the solution was determined primarily by the observed magnitudes.

4. Rat Island Earthquake of the 15th of May 1966. All the observed first motion consisted of compressions. Figure 7 shows the observed radiation pattern. The calculated radiation pattern was also governed mainly by the magnitudes in this case, since the strike angle could be varied considerably without changing any of the signs of the first motion. 84 stations were used, of which 21 reported magnitudes and the rest only first motions. The results are given in Figure 8 and Table 7. This was another case where many of the stations were close to nodes and hence the new value of  $m_b = 5.96$  as against the C&GS value of 5.8 reflects this.

5. Rat Island Earthquake of the 4th of July 1966. Figure 9 shows the observed radiation pattern. This is a more complicated source mechanism and hence the final score 80-18 shows

that the fit was not too good. 22 stations reported magnitudes and the rest reported first motions only. One of the difficulties was that no magnitudes were reported in the second quadrant, thus missing an entire lobe of the pattern. The results are shown in Figure 10 and Table 8.

6. Rat Island Earthquake of the 22nd of November 1965. This was another case of compressions only, with no stations reporting magnitudes in the second and third quadrant. Figure 11 shows the observed radiation pattern. A change of  $30^\circ$  in the strike angle did not change any of the first motion directions. The results are given in Figure 12 and Table 9.

Another run was made using additional magnitudes supplied by D. Lambert of SDL in a private communication. The new observed radiation pattern is given in Figure 13. For this case, there were magnitudes observed in the third quadrant, but not in the second quadrant. The strike direction did not change, but the dip and slip angles, and hence the second solution, did change somewhat. The results are given in Figure 14 and Table 10.

7. Hindu-Kush Earthquake of the 28th of January 1964. This was a complicated source mechanism. The observed radiation pattern is given in Figure 15. Values of  $\log_{10} A/T$  were taken from the ISC bulletin and for the first motion, only those stations used by Hirasawa and Hedayati (1966) were included. The solution favours the one obtained by Ritsema (1966). The final score of 53-14 reflects the inadequacy of the solution. Again, one of the difficulties is that there are no magnitudes observed between  $115^\circ$  and  $295^\circ$  azimuth. The results are shown in Figure 16 and Table 11.

8. Alaskan Earthquake of the 28th of March 1964 (main shock). The 22 values of magnitude for this event were taken from the ISC bulletin and signs of first motion were taken from the bulletin and the C&GS Earthquake Data Reports. The observed radiation pattern is given in Figure 17. The final score obtained, 86-22, suggests that quite a few of the stations reported erroneous first motions, since the solution agrees quite well with that of Stauder and Bollinger (1956). The results are given in Figure 18 and Table 12.

Another run was made using additional first motions supplied by Harding in a preprint of the C&GS on the Prince William Sound Earthquakes (1968). The solution was improved considerably and the final score was 134-17. The results are shown in Figure 19 and Table 13.

9. The Niigata Earthquake of the 16th of June 1964. This was another case where  $m_b$  given by the C&GS was too low and the new value of 6.5 as against 6.1 is correcting in the right direction. The observed radiation pattern is given in Figure 20. The results, shown in Figure 21 and Table 14, do not agree very well with the solution found by Hirasawa (1965).



## CONCLUSIONS

Comparison of the fault plane solutions obtained by the new method and those obtained using first motions only show that indeed it is possible to find reasonable agreement. The solution of the Hindu-Kush earthquake parameters show that although better agreement with the first motion directions was obtained by Hedayati and Hirasawa (1966), the amplitude radiation pattern does not agree as well with the observed pattern as that obtained by using a combination of first motion directions together with observed body-wave magnitudes.

The results of the Rat Island earthquake of the 5th of February, 1965 show that the proposed method compensates correctly where too many of the observed magnitudes were near to nodes. This shows that the proposed definition of magnitude is superior to taking the arithmetic mean of the observations of  $m_b$ .

The fault plane solution found by this method is probably not as accurate as that obtained by S-wave data. However, the new method gives two checks on the accuracy obtained, the first by simply the number of differences in sign between calculated and observed, i.e., the "score". The second is by examining the confidence limits of the magnitude.

The results also indicate that in order to take the radiation pattern into account when finding the "true" value of  $m_b$ , it is sufficient to use an approximate solution to the source parameters. This is possible by using readily available magnitude and first motion data without laboriously having to re-examine records.

### Suggestions for Future Research

1. In order to make best use of the method outlined above,

there still remains to be determined the minimum number of input data which must be used in order to get a good solution. For the cases tried here, rather more points were used than really necessary.

2. Instead of the equal weights least squares solution, it might be possible to get some improvement by using a weighted least squares procedure.

3. If more emphasis is to be placed on the accuracy of the fault plane solution obtained using the new method discussed above, it is possible to add the S-wave data to the least-squares procedure.

4. A still better way to define the "magnitude" of an event may be to use the idea of moment, e.g., Aki (1966).

#### ACKNOWLEDGEMENTS

The author wishes to thank Dr. E. A. Flinn for helpful discussions and encouragement in this project, Dr. T. Cohen who helped collect the data from the film records of the observatories, Dr. K. Shumway who suggested how to obtain statistical estimates of the accuracy of the results, the Rev. W. Stauder for supplying the first motion data for the Rat Island sequence, Mr. S. Harding for the preprint of the forthcoming publication of the Prince William Sound earthquakes and the much appreciated cooperation of the C&GS in this project.

## REFERENCES

- Aki, K., Generation and Propagation of G Waves from the Niigata Earthquake of June 16, 1964, Pt. 1. A Statistical Analysis. Pt 2. Estimation of Earthquake Moment, Released Energy, and Stress-Strain Drop from the G Wave Spectrum, Bull. Earthq. Res. Inst. Tokyo, 44, 23-72, 73-88, 1966.
- Algermissen, S.T., S.T. Harding and R.W. Sherburne, The hypocenter, origin time, and magnitude of the Prince William Sound earthquake of March 28, 1964 (in press).
- Gutenberg, B. and C.F. Richter, Magnitude and energy of earthquakes, Ann. di Geofis. 9, 1-15 (1956).
- Harding, S.T., and S.T. Algermissen, The Focal Mechanism of the Prince William Sound Earthquake of March 28, 1964, and Related Earthquakes (in press).
- Hedayati, A. and T. Hirasawa, Mechanism of the Hindu-Kush earthquake of January 28, 1964, derived from S wave data: the use of pP phase for the focal mechanism determination, Bull. Earthqu. Res. Inst. Tokyo, 44, 1419 - 1434, 1966.
- Hirasawa, T., Source Mechanism of the Niigata Earthquake of June 16, 1964, as derived from body waves, Jour. Phys. Earth 13, 35-66 (1965).
- Menahem, B.A., S.W. Smith and T.L. Teng, A procedure for source studies from spectrum of long period seismic body waves, Bull. Seismol. Soc. Am., 55, 203-235, 1964.
- Ritsema, A.R., The fault-plane solutions of earthquakes of the Hindu-Kush Centre, Tectonophysics 3, 147-163, 1966.



- Stauder, W. and G.A. Bollinger, The S Wave project for focal mechanism studies - Earthquakes of 1962, Bull. Seismol. Soc. Am., 54, 2199-2208, 1964.
- Stauder, W., S.J. and O. Nuttli, Investigation of phase velocities of long period surface waves and focal mechanism studies, Final Report August 1, 1960 - August 31, 1965, AFCRL Project Vela-Uniform (1965).
- Stauder, W. and G.A. Bollinger, The focal mechanism of the Alaska earthquake of March 28, 1964 and of its after-shock sequence, Geo. Phys. Res., 71, 5283-5296, 1966.
- Stauder, W., Mechanism of the Rat Island earthquake sequence of February 4, 1964 with relation to island arcs and sea-floor spreading, Geo. Phys. Res., 73, 3847-3858, 1968.
- Teng, T.L. and A. Ben Menahem, Mechanisms of deep earthquakes from spectrums of isolated body-wave signals, Geo. Phys. Res., 70, 5157-5170, 1965.

TABLE 1

## Solution Using The New Method

NO.	DATE	PLANE 1				PLANE 2				C&GS m <sub>b</sub>	MEAN CORRECTED m <sub>b</sub>	90% CONFIDENCE	
		DIP DIR.	DIP	SLIP	DIP DIR.	OIP	SLIP	SCORE	UPPER LIMIT			LOWER LIMIT	
1	Mar 21, 1964	185°	86°	300°	89°	31°	172°	37-1	5.8	5.84	6.0	5.6	
2	Feb 5, 1965	145°	82°	100°	17°	12°	38°	72-12	5.9	6.28	6.4	6.0	
3	Oct 1, 1965	215°	40°	290°	241°	53°	106°	80-0	6.3	6.36	6.5	6.0	
4	May 15, 1966	105°	50°	100°	301°	41°	78°	84-0	5.8	5.96	6.2	5.6	
5	Jul 4, 1966	280°	84°	350°	189°	81°	173°	80-18	6.2	6.15	6.4	5.6	
6	Nov 22, 1965	180°	60°	80°	341°	31°	106°	66-2	5.9	5.78	5.9	5.6	
		180°	50°	70°	331°	43°	112°	88-3		6.07	6.2	6.0	
7	Jan 28, 1964	90°	70°	170°	357°	80°	20°	53-14	6.1	6.39	6.5	6.1	
8	Mar 28, 1964	135°	80°	30°	231°	61°	168°	86-22	8.5*	7.26	7.6	-	
		340°	86°	200°	71°	71°	4°	134-17		7.25	7.4	6.9	
9	Jun 16, 1967	135°	60°	140°	23°	56°	37°	71-9	6.1	6.53	6.7	6.1	

\*The observed values of  $m_b$  were too small, the value of 8.5 is not based on them.

TABLE 2  
Results Previously Obtained

NO.	DATE	PLANE 1				PLANE 2				SCORE	SOURCE
		OIP	OIR.	OIP	SLIP	OIP	OIR.	OIP	SLIP		
1	Mar 21, 1964	175°		84°	315°						Ben Menahem et al (1965)
2	Feb 5, 1965	141°		75°		325°		15°		63-0	Stauder (1968)
3	Oct 1, 1965	175°		50°		40°		50°		74-0	Stauder (1968)
4	May 15, 1966 Alternate	136° 145°		61° 75°		349° 13°		34° 22°		67-0 67-0	Stauder (1968) Stauder (1968)
5	Jul 4, 1966	97°		85°		187°		85°		70-1	Stauder (1968)
6	Nov 22, 1965	145°		70°		354°		22°		56-0	Stauder (1968) Hedayati & Hirasawa (1966)
7	Jan 28, 1964	-35.2° ± 12.8° -37.5° ± 12.8° -118° -64° -40° -70°		21.3° ± 4.3° 21.9° ± 4.2° 25° 22° 28° 70°	63.0° ± 12.1° 65.0° ± 11.9° 54.5° 90° 90°	116.1° ± 3.8° 115.8° ± 3.7° 100° 116° 140° 110°		71.1° ± 2.0° 70.3° ± 2.1° 70° 68° 62° 20°	80.0° ± 4.1° 80.4° ± 4.0° 75° 90° 90°		L.S. Sol. (1) L.S. Sol. (2) Graph. Sol. (1) Graph. Sol. (2) Ritsema (1966) Aki (1966)
8	Mar 28, 1964	152° 152° 310° 135°		32° 82° 87° 62°		332° 248° 220° 45°		8° 52° 80° 90°			Harding (1968) Harding (1968) Harding (1968) Harding (1968)
9	Jun 16, 1964	101.7° ± 13.9°		31.2° ± 1.4°	88.6° ± 9.8°	-79.9° ± 5.1°		58.8° ± 1.3°	89.2° ± 7.9°		Hirasawa (1965)

Table 3. Example of Input Data for the Banda Sea Earthquake of 21 March 1964.

EQU. BANDA SEA, 21 MARCH, 1964, M=3.7MM, M=5.8									
37	1	367.0	00.0	5.0	5				
1	STA(1)	LIC(1)							
1	ABU	41.70	130.01	100.00	100.00	100.00	100.00	100.00	100.00
2	COL	93.34	157.50	100.00	100.00	100.00	100.00	100.00	100.00
3	KIP	77.65	157.05	100.00	100.00	100.00	100.00	100.00	100.00
4	PMG	14.27	124.19	100.00	100.00	100.00	100.00	100.00	100.00
5	HIV	34.70	135.30	100.00	100.00	100.00	100.00	100.00	100.00
6	CAN	34.65	135.36	100.00	100.00	100.00	100.00	100.00	100.00
7	NLA	20.20	131.27	100.00	100.00	100.00	100.00	100.00	100.00
8	LUN	102.17	150.00	100.00	100.00	100.00	100.00	100.00	100.00
9	KUN	100.25	150.00	100.00	100.00	100.00	100.00	100.00	100.00
10	REV	94.80	157.90	100.00	100.00	100.00	100.00	100.00	100.00
11	SAG	23.85	129.35	100.00	100.00	100.00	100.00	100.00	100.00
12	ANP	32.05	134.32	100.00	100.00	100.00	100.00	100.00	100.00
13	MAT	43.70	130.04	100.00	100.00	100.00	100.00	100.00	100.00
14	MTJ	43.90	130.07	100.00	100.00	100.00	100.00	100.00	100.00
15	GUA	20.04	131.12	100.00	100.00	100.00	100.00	100.00	100.00
16	MOR	77.54	153.02	100.00	100.00	100.00	100.00	100.00	100.00
17	HAB	24.27	129.77	100.00	100.00	100.00	100.00	100.00	100.00
18	MNH	31.00	134.25	100.00	100.00	100.00	100.00	100.00	100.00
19	AFI	54.70	145.06	100.00	100.00	100.00	100.00	100.00	100.00
20	LUG	34.50	137.30	100.00	100.00	100.00	100.00	100.00	100.00
21	PVC	41.00	137.50	100.00	100.00	100.00	100.00	100.00	100.00
22	KCU	37.94	134.08	100.00	100.00	100.00	100.00	100.00	100.00
23	NCU	40.40	137.02	100.00	100.00	100.00	100.00	100.00	100.00
24	CTA	22.42	127.92	100.00	100.00	100.00	100.00	100.00	100.00
25	PHS	31.57	134.11	100.00	100.00	100.00	100.00	100.00	100.00
26	REL	54.21	143.18	100.00	100.00	100.00	100.00	100.00	100.00
27	TAL	40.20	137.50	100.00	100.00	100.00	100.00	100.00	100.00
28	ACE	30.17	133.35	100.00	100.00	100.00	100.00	100.00	100.00
29	HUN	27.60	132.11	100.00	100.00	100.00	100.00	100.00	100.00
30	PRE	95.97	157.39	100.00	100.00	100.00	100.00	100.00	100.00
31	FUL	90.40	157.35	100.00	100.00	100.00	100.00	100.00	100.00
32	SHI	80.57	154.23	100.00	100.00	100.00	100.00	100.00	100.00
33	IST	100.25	150.00	100.00	100.00	100.00	100.00	100.00	100.00
34	SIL	47.27	140.13	100.00	100.00	100.00	100.00	100.00	100.00
35	MAY	21.90	127.49	100.00	100.00	100.00	100.00	100.00	100.00
36	MIC	31.57	134.11	100.00	100.00	100.00	100.00	100.00	100.00
37	SEO	43.70	130.07	100.00	100.00	100.00	100.00	100.00	100.00

Table 4. Results for the Banda Sea Earthquake of  
21 March 1964.

$\bar{M} = 2.4467E 02$   $\text{CONV} = 1.1502E 02$   $\text{MEAN MAG} = 5.45$   
 95 PERCENT CONF. UPPER LIMIT = 4.0  
 95 PERCENT CONF. LOWER LIMIT = 5.6  
 SAMPLE VARIANCE = 3.2120E 03

1	STA(1)	AZ(1)	CALC. MAG(1)	C/U	MRS. MAG(1)	C/U
1	ARU	9.0	6.0	-	6.4	-
2	COL	25.0	5.9	-	5.3	-
3	KIP	67.0	5.8	-	5.7	-
4	PMG	100.0	4.9	+	5.8	+
5	RIV	145.0	6.0	+	6.1	+
6	CAN	149.0	6.0	+	5.9	+
7	NMA	315.0	5.5	-	5.3	-
8	NUR	330.0	5.8	-	5.2	-
9	KJN	334.0	5.8	-	5.7	-
10	KEV	340.0	5.8	-	5.5	-
11	BAG	342.0	5.8	-	5.3	-
12	ANP	349.0	5.9	-	6.0	-
13	MAT	12.0	6.1	-	0	-
14	MTJ	14.3	6.1	-	0	-
15	GUA	40.3	6.1	-	0	-
16	HON	66.0	5.8	-	0	-
17	HAB	86.0	5.6	-	0	-
18	HNR	97.3	4.6	-	0	-
19	AFI	102.3	4.5	+	0	-
20	LUG	106.0	5.3	+	0	+
21	PVC	109.7	5.5	+	0	+
22	KOU	115.4	5.6	+	0	+
23	NOU	117.1	5.7	+	0	+
24	CTA	129.1	5.9	+	0	+
25	HRS	134.3	6.0	+	0	+
26	WEL	137.3	5.9	+	0	+
27	TAU	157.0	6.0	+	0	+
28	ADE	162.1	6.1	+	0	+
29	MUN	201.0	5.9	+	0	+
30	PRE	243.3	5.3	+	0	+
31	BUL	248.4	5.2	+	0	+
32	SHI	301.4	5.6	-	0	-
33	ISI	310.3	5.6	-	0	-
34	SWL	313.7	5.6	-	0	-
35	MAN	342.1	5.8	-	0	-
36	MKC	335.2	5.8	-	0	-
37	SEO	358.4	6.0	-	0	-

Table 5. Results for the Rat Island Earthquake of 5 February 1964.

MEAN 2.5MMAS UP CORVA 3.02276 UP MEAN MAGN 0.70  
 95 PERCENT CONF. UPPER LIMIT 4.4  
 95 PERCENT CONF. LOWER LIMIT 0.0  
 SAMPLE VARIANCE 3.4350E 04

STATION	4/11	UPPER	LOWER	CONF.	C/U
1 LUC	29.1	0.3	0	0.1	0
2 LUC	37.4	0.3	0	0.3	0
3 LUC	59.7	0.3	0	0.4	0
4 WMO	69.0	0.3	0	0.6	0
5 WMO	71.3	0.3	0	0.8	0
6 ALU	74.2	0.3	0	0.6	0
7 IFU	74.1	0.3	0	0.3	0
8 WIG	209.0	0.3	0	0.6	0
9 DAV	239.4	0.3	0	0.8	0
10 PAG	250.3	0.3	0	0.0	0
11 NUK	301.7	0.3	0	0.2	0
12 NUK	344.0	0.3	0	0.8	0
13 STU	349.4	0.3	0	0.0	0
14 NOM	2.2	0.3	0	0	0
15 VAL	2.4	0.3	0	0	0
16 ARU	5.8	0.3	0	0	0
17 ALF	9.4	0.3	0	0	0
18 GIM	19.1	0.3	0	0	0
19 NPS	24.1	0.3	0	0	0
20 COL	42.1	0.3	0	0	0
21 MNT	45.3	0.3	0	0	0
22 RPU	47.2	0.3	0	0	0
23 ORU	48.9	0.3	0	0	0
24 SCP	51.1	0.3	0	0	0
25 AAN	53.7	0.3	0	0	0
26 RLA	55.2	0.3	0	0	0
27 SJP	55.7	0.3	0	0	0
28 MDS	56.2	0.3	0	0	0
29 CSC	57.7	0.3	0	0	0
30 ATL	60.3	0.3	0	0	0
31 FLO	60.5	0.3	0	0	0
32 CAN	60.6	0.3	0	0	0
33 RKF	63.4	0.3	0	0	0
34 RCU	63.8	0.3	0	0	0
35 M07	67.1	0.3	0	0	0
36 SPU	67.2	0.3	0	0	0
37 DAL	69.2	0.3	0	0	0
38 GOL	69.3	0.3	0	0	0
39 LIW	72.2	0.3	0	0	0
40 JCI	73.1	0.3	0	0	0
41 TUC	79.9	0.3	0	0	0
42 GSC	81.0	0.3	0	0	0
43 MIV	109.1	0.3	0	0	0
44 NAM	205.9	0.3	0	0	0
45 CTA	207.1	0.3	0	0	0
46 NAM	248.7	0.3	0	0	0
47 ANP	250.5	0.3	0	0	0
48 NHA	257.5	0.3	0	0	0
49 HMC	260.0	0.3	0	0	0
50 SEO	264.7	0.3	0	0	0
51 CHU	270.4	0.3	0	0	0
52 SML	280.7	0.3	0	0	0
53 MGV	281.1	0.3	0	0	0
54 RNU	281.6	0.3	0	0	0
55 POJ	289.5	0.3	0	0	0
56 ADI	293.5	0.3	0	0	0
57 LAM	297.4	0.3	0	0	0
58 SHI	311.9	0.3	0	0	0
59 TEM	315.4	0.3	0	0	0
60 JFN	320.1	0.3	0	0	0
61 INI	334.3	0.3	0	0	0
62 ATU	337.1	0.3	0	0	0
63 WCU	341.5	0.3	0	0	0
64 ANU	345.4	0.3	0	0	0
65 THJ	346.3	0.3	0	0	0
66 REV	346.4	0.3	0	0	0
67 HMC	347.2	0.3	0	0	0
68 COP	349.3	0.3	0	0	0
69 KGN	351.2	0.3	0	0	0
70 GSN	358.5	0.3	0	0	0
71 TOL	358.7	0.3	0	0	0
72 HAL	359.0	0.3	0	0	0



Table 6. Results for the Rat Island Earthquake of 1 October 1965.

X<sub>0</sub> = 4.7195 02 000000 0.0000 02 MEAN MAG = 5.30  
 95 PERCENT CONF. UPPER LIMIT = 4.5  
 95 PERCENT CONF. LOWER LIMIT = 4.0  
 SAMPLE VARIANCE = 5.077AE 04

I	STATION	AZIM	CALC.		OBS.	C/U
			MAG(1)	MAG(2)		
1	NDH	2.0	5.7	-	5.3	-
2	ALH	9.5	5.5	-	5.0	-
3	KTH	7.8	5.0	-	6.0	-
4	GDH	20.0	5.0	-	6.0	-
5	MHC	21.4	5.0	-	6.2	-
6	TRH	50.0	6.4	-	6.1	-
7	CPH	61.5	6.3	-	5.0	-
8	ATL	62.3	6.3	-	6.1	-
9	CAR	64.1	6.4	-	6.4	-
10	WHO	70.5	6.3	-	6.0	-
11	HRU	72.0	6.3	-	6.3	-
12	JCT	74.0	6.4	-	6.4	-
13	ALH	75.4	6.3	-	5.9	-
14	TFO	79.2	6.3	-	5.3	-
15	HKS	82.0	6.3	-	7.1	-
16	PHG	214.2	6.4	-	5.7	-
17	RAG	255.4	6.3	-	6.2	-
18	RAG	255.4	6.3	-	5.5	-
19	POH	292.7	6.4	-	6.4	-
20	NUH	346.2	6.1	-	6.5	-
21	PRH	349.4	6.2	-	6.0	-
22	MOZ	351.4	6.2	-	6.1	-
23	GOP	351.7	6.2	-	6.4	-
24	STU	352.0	6.2	-	6.2	-
25	KUL	353.2	6.2	-	4.4	-
26	ESR	.0	6.2	-	0	-
27	HAL	2.1	6.3	-	0	-
28	PTU	5.1	6.3	-	0	-
29	VAL	5.3	6.2	-	0	-
30	AKU	7.4	6.0	-	0	-
31	CHC	35.0	5.6	-	0	-
32	MNT	46.0	6.2	-	0	-
33	VEN	47.7	6.2	-	0	-
34	RFC	49.0	6.3	-	0	-
35	GRU	50.7	6.3	-	0	-
36	SCP	52.0	6.3	-	0	-
37	AAM	55.1	6.3	-	0	-
38	MDS	57.7	6.2	-	0	-
39	EDH	58.1	6.1	-	0	-
40	BJP	58.0	6.4	-	0	-
41	FLO	61.0	6.3	-	0	-
42	OXF	64.7	6.3	-	0	-
43	SPH	67.5	6.2	-	0	-
44	GOL	70.1	6.3	-	0	-
45	DAL	70.0	6.3	-	0	-
46	LON	71.0	6.2	-	0	-
47	LUN	73.5	6.3	-	0	-
48	DUG	74.1	6.3	-	0	-
49	COM	74.0	6.3	-	0	-
50	HMP	74.0	6.4	-	0	-
51	OUI	70.0	6.5	-	0	-
52	TUC	80.7	6.4	-	0	-
53	GSC	81.0	6.3	-	0	-
54	RAH	198.0	6.5	-	0	-
55	WFL	192.0	6.5	-	0	-
56	CTA	211.0	6.4	-	0	-
57	ADP	211.5	6.5	-	0	-
58	NUH	222.4	6.4	-	0	-
59	DAV	244.2	6.3	-	0	-
60	UND	250.0	6.4	-	0	-
61	NMA	261.7	6.3	-	0	-
62	ANP	261.0	6.2	-	0	-
63	HRC	265.4	6.3	-	0	-
64	SEO	271.0	6.2	-	0	-
65	SML	284.5	6.3	-	0	-
66	KOU	284.7	6.4	-	0	-
67	NUI	296.5	6.3	-	0	-
68	LAH	300.7	6.3	-	0	-
69	QUE	304.0	6.3	-	0	-
70	SWI	314.0	6.3	-	0	-
71	THH	319.0	6.3	-	0	-
72	TAN	323.0	6.3	-	0	-
73	JEH	329.7	6.3	-	0	-
74	UIN	336.7	6.3	-	0	-
75	IST	337.0	6.3	-	0	-
76	ATH	340.1	6.3	-	0	-
77	REV	349.7	6.3	-	0	-
78	TRI	349.1	6.2	-	0	-
79	RMC	349.0	6.2	-	0	-
80	RTN	353.7	6.1	-	0	-

Table 7. Results for the Rat Island Earthquake of 15 May 1966.

NO. 2, 4, 7, 10, 13, 16, 19, 22, 25, 28, 31, 34, 37, 40, 43, 46, 49, 52, 55, 58, 61, 64, 67, 70, 73, 76, 79, 82, 85, 88, 91, 94, 97, 100, 103, 106, 109, 112, 115, 118, 121, 124, 127, 130, 133, 136, 139, 142, 145, 148, 151, 154, 157, 160, 163, 166, 169, 172, 175, 178, 181, 184, 187, 190, 193, 196, 199, 202, 205, 208, 211, 214, 217, 220, 223, 226, 229, 232, 235, 238, 241, 244, 247, 250, 253, 256, 259, 262, 265, 268, 271, 274, 277, 280, 283, 286, 289, 292, 295, 298, 301, 304, 307, 310, 313, 316, 319, 322, 325, 328, 331, 334, 337, 340, 343, 346, 349, 352, 355, 358, 361, 364, 367, 370, 373, 376, 379, 382, 385, 388, 391, 394, 397, 400, 403, 406, 409, 412, 415, 418, 421, 424, 427, 430, 433, 436, 439, 442, 445, 448, 451, 454, 457, 460, 463, 466, 469, 472, 475, 478, 481, 484, 487, 490, 493, 496, 499, 502, 505, 508, 511, 514, 517, 520, 523, 526, 529, 532, 535, 538, 541, 544, 547, 550, 553, 556, 559, 562, 565, 568, 571, 574, 577, 580, 583, 586, 589, 592, 595, 598, 601, 604, 607, 610, 613, 616, 619, 622, 625, 628, 631, 634, 637, 640, 643, 646, 649, 652, 655, 658, 661, 664, 667, 670, 673, 676, 679, 682, 685, 688, 691, 694, 697, 700, 703, 706, 709, 712, 715, 718, 721, 724, 727, 730, 733, 736, 739, 742, 745, 748, 751, 754, 757, 760, 763, 766, 769, 772, 775, 778, 781, 784, 787, 790, 793, 796, 799, 802, 805, 808, 811, 814, 817, 820, 823, 826, 829, 832, 835, 838, 841, 844, 847, 850, 853, 856, 859, 862, 865, 868, 871, 874, 877, 880, 883, 886, 889, 892, 895, 898, 901, 904, 907, 910, 913, 916, 919, 922, 925, 928, 931, 934, 937, 940, 943, 946, 949, 952, 955, 958, 961, 964, 967, 970, 973, 976, 979, 982, 985, 988, 991, 994, 997, 1000.

1	STATION	AZIMUTH	DIP	SLIP	CMF	CMZ
1	NOM	3.2	6.0	0	5.5	0
2	ATG	7.2	6.1	0	5.4	0
3	MHC	21.5	6.0	0	5.4	0
4	WPC	21.5	6.0	0	5.7	0
5	WPC	21.5	6.0	0	5.6	0
6	WPC	21.5	6.0	0	5.6	0
7	CHI	17.5	5.7	0	5.7	0
8	CHI	17.5	5.7	0	5.7	0
9	CHI	17.5	5.7	0	5.7	0
10	CHI	17.5	5.7	0	5.7	0
11	CHI	17.5	5.7	0	5.7	0
12	CHI	17.5	5.7	0	5.7	0
13	CHI	17.5	5.7	0	5.7	0
14	CHI	17.5	5.7	0	5.7	0
15	CHI	17.5	5.7	0	5.7	0
16	CHI	17.5	5.7	0	5.7	0
17	CHI	17.5	5.7	0	5.7	0
18	CHI	17.5	5.7	0	5.7	0
19	CHI	17.5	5.7	0	5.7	0
20	CHI	17.5	5.7	0	5.7	0
21	CHI	17.5	5.7	0	5.7	0
22	CHI	17.5	5.7	0	5.7	0
23	CHI	17.5	5.7	0	5.7	0
24	CHI	17.5	5.7	0	5.7	0
25	CHI	17.5	5.7	0	5.7	0
26	CHI	17.5	5.7	0	5.7	0
27	CHI	17.5	5.7	0	5.7	0
28	CHI	17.5	5.7	0	5.7	0
29	CHI	17.5	5.7	0	5.7	0
30	CHI	17.5	5.7	0	5.7	0
31	CHI	17.5	5.7	0	5.7	0
32	CHI	17.5	5.7	0	5.7	0
33	CHI	17.5	5.7	0	5.7	0
34	CHI	17.5	5.7	0	5.7	0
35	CHI	17.5	5.7	0	5.7	0
36	CHI	17.5	5.7	0	5.7	0
37	CHI	17.5	5.7	0	5.7	0
38	CHI	17.5	5.7	0	5.7	0
39	CHI	17.5	5.7	0	5.7	0
40	CHI	17.5	5.7	0	5.7	0
41	CHI	17.5	5.7	0	5.7	0
42	CHI	17.5	5.7	0	5.7	0
43	CHI	17.5	5.7	0	5.7	0
44	CHI	17.5	5.7	0	5.7	0
45	CHI	17.5	5.7	0	5.7	0
46	CHI	17.5	5.7	0	5.7	0
47	CHI	17.5	5.7	0	5.7	0
48	CHI	17.5	5.7	0	5.7	0
49	CHI	17.5	5.7	0	5.7	0
50	CHI	17.5	5.7	0	5.7	0
51	CHI	17.5	5.7	0	5.7	0
52	CHI	17.5	5.7	0	5.7	0
53	CHI	17.5	5.7	0	5.7	0
54	CHI	17.5	5.7	0	5.7	0
55	CHI	17.5	5.7	0	5.7	0
56	CHI	17.5	5.7	0	5.7	0
57	CHI	17.5	5.7	0	5.7	0
58	CHI	17.5	5.7	0	5.7	0
59	CHI	17.5	5.7	0	5.7	0
60	CHI	17.5	5.7	0	5.7	0
61	CHI	17.5	5.7	0	5.7	0
62	CHI	17.5	5.7	0	5.7	0
63	CHI	17.5	5.7	0	5.7	0
64	CHI	17.5	5.7	0	5.7	0
65	CHI	17.5	5.7	0	5.7	0
66	CHI	17.5	5.7	0	5.7	0
67	CHI	17.5	5.7	0	5.7	0
68	CHI	17.5	5.7	0	5.7	0
69	CHI	17.5	5.7	0	5.7	0
70	CHI	17.5	5.7	0	5.7	0
71	CHI	17.5	5.7	0	5.7	0
72	CHI	17.5	5.7	0	5.7	0
73	CHI	17.5	5.7	0	5.7	0
74	CHI	17.5	5.7	0	5.7	0
75	CHI	17.5	5.7	0	5.7	0
76	CHI	17.5	5.7	0	5.7	0
77	CHI	17.5	5.7	0	5.7	0
78	CHI	17.5	5.7	0	5.7	0
79	CHI	17.5	5.7	0	5.7	0
80	CHI	17.5	5.7	0	5.7	0
81	CHI	17.5	5.7	0	5.7	0
82	CHI	17.5	5.7	0	5.7	0
83	CHI	17.5	5.7	0	5.7	0
84	CHI	17.5	5.7	0	5.7	0
85	CHI	17.5	5.7	0	5.7	0
86	CHI	17.5	5.7	0	5.7	0
87	CHI	17.5	5.7	0	5.7	0
88	CHI	17.5	5.7	0	5.7	0
89	CHI	17.5	5.7	0	5.7	0
90	CHI	17.5	5.7	0	5.7	0
91	CHI	17.5	5.7	0	5.7	0
92	CHI	17.5	5.7	0	5.7	0
93	CHI	17.5	5.7	0	5.7	0
94	CHI	17.5	5.7	0	5.7	0
95	CHI	17.5	5.7	0	5.7	0
96	CHI	17.5	5.7	0	5.7	0
97	CHI	17.5	5.7	0	5.7	0
98	CHI	17.5	5.7	0	5.7	0
99	CHI	17.5	5.7	0	5.7	0
100	CHI	17.5	5.7	0	5.7	0



Table 8. Results for the Rat Island Earthquake of 4 July 1966.

MEAN 1.5150E-04 UNITS/SEC 1.0000E-04 SEAN MAGN 0.10  
 95 PERCENT CONF. UPPER LIMIT 4.4  
 95 PERCENT CONF. LOWER LIMIT 0.4  
 SAMPLE VARIANCE 2.4183E-08

STATION	AMPL	PERC	PERC	PERC	PERC
1	2	3	4	5	6
1 ALP	10.0	5.7	*	5.4	*
2 MHC	22.4	6.2	*	6.0	*
3 HPC	27.2	6.2	*	5.8	*
4 CMC	37.4	6.3	*	5.7	*
5 BIA	58.0	5.9	*	6.4	*
6 SJG	60.4	5.4	*	6.2	*
7 THH	60.7	5.2	*	5.9	*
8 CPU	63.2	5.9	*	5.9	*
9 CAM	65.3	5.9	*	6.8	*
10 LAU	65.5	6.2	*	5.0	*
11 SPD	70.1	6.1	*	6.4	*
12 MHO	72.5	5.8	*	6.9	*
13 UHO	74.9	5.9	*	6.5	*
14 DUB	76.0	5.9	*	6.0	*
15 ALU	77.0	5.7	*	6.3	*
16 THH	81.0	5.4	*	5.9	*
17 HAH	212.2	5.0	*	5.6	*
18 PHG	215.4	5.9	*	6.5	*
19 PDD	223.4	5.5	*	6.9	*
20 QUE	365.0	4.2	*	5.8	*
21 COP	352.6	5.8	*	6.9	*
22 STU	353.7	4.4	*	5.1	*
23 ESK	1.7	5.1	*	U	*
24 NOH	3.3	5.1	*	U	*
25 HAL	3.5	5.2	*	U	*
26 KTD	6.4	5.3	*	U	*
27 VAL	6.5	5.4	*	U	*
28 KTG	6.6	5.6	*	U	*
29 PDA	20.0	5.6	*	U	*
30 GDM	20.9	6.0	*	U	*
31 COL	39.1	6.5	*	U	*
32 MES	49.2	6.6	*	U	*
33 HEC	51.1	5.8	*	U	*
34 SCP	54.9	6.0	*	U	*
35 HRR	56.0	6.0	*	U	*
36 AAM	56.6	6.0	*	U	*
37 SJP	60.2	5.5	*	U	*
38 SLH	63.0	6.0	*	U	*
39 ROL	65.4	5.9	*	U	*
40 HMI	67.5	6.0	*	U	*
41 SPA	68.5	5.7	*	U	*
42 BOZ	69.7	6.1	*	U	*
43 GOL	72.5	6.0	*	U	*
44 LON	73.7	6.1	*	U	*
45 HON	74.5	5.2	*	U	*
46 HMP	76.2	5.2	*	U	*
47 JCI	76.8	5.5	*	U	*
48 COH	77.0	5.9	*	U	*
49 LPS	80.3	5.4	*	U	*
50 QHI	81.0	5.5	*	U	*
51 THH	83.0	5.1	*	U	*
52 HNV	83.2	5.5	*	U	*
53 TAL	84.0	5.5	*	U	*
54 GIP	86.0	5.4	*	U	*
55 KIP	142.1	6.6	*	U	*
56 AFI	171.3	6.3	*	U	*
57 MVM	262.1	4.5	*	U	*
58 RTV	463.0	5.2	*	U	*
59 CTA	472.5	5.6	*	U	*
60 GUA	229.3	6.3	*	U	*
61 DAV	245.0	6.3	*	U	*
62 HNH	251.0	6.6	*	U	*
63 HAN	254.1	5.3	*	U	*
64 HAN	255.6	6.3	*	U	*
65 ANP	262.0	6.3	*	U	*
66 HED	265.3	6.4	*	U	*
67 HRC	265.7	6.2	*	U	*
68 SEU	270.2	6.3	*	U	*
69 HON	285.5	5.5	*	U	*
70 NDI	297.5	5.4	*	U	*
71 LAN	301.5	4.9	*	U	*
72 SHI	316.0	5.0	*	U	*
73 JES	320.0	5.1	*	U	*
74 HLE	333.0	5.1	*	U	*
75 ISI	334.5	5.2	*	U	*
76 ATU	341.5	5.1	*	U	*
77 TPI	351.0	4.4	*	U	*
78 HPL	354.3	4.2	*	U	*
79 PGI	354.7	4.9	*	U	*
80 GVS	355.3	3.5	*	U	*

**Table 9. Results for the Rat Island Earthquake of 22 November 1965.**

20	1.92000	02	010000	4.00000	01	0000	0.000
05	PERCENT CONF.	UPPER LIMIT	4.4				
05	PERCENT CONF.	LOWER LIMIT	0.0				
SAMPLE VARIANCE 1.00000							
1	010111	02111	03111	04111	05111	06111	07111
1	000	3.3	3.0	•	3.7	•	•
2	010	0.7	3.0	•	3.7	•	•
3	010	0.7	3.0	•	3.7	•	•
4	010	0.7	3.0	•	3.7	•	•
5	010	0.7	3.0	•	3.7	•	•
6	010	0.7	3.0	•	3.7	•	•
7	010	0.7	3.0	•	3.7	•	•
8	010	0.7	3.0	•	3.7	•	•
9	010	0.7	3.0	•	3.7	•	•
10	010	0.7	3.0	•	3.7	•	•
11	010	0.7	3.0	•	3.7	•	•
12	010	0.7	3.0	•	3.7	•	•
13	010	0.7	3.0	•	3.7	•	•
14	010	0.7	3.0	•	3.7	•	•
15	010	0.7	3.0	•	3.7	•	•
16	010	0.7	3.0	•	3.7	•	•
17	010	0.7	3.0	•	3.7	•	•
18	010	0.7	3.0	•	3.7	•	•
19	010	0.7	3.0	•	3.7	•	•
20	010	0.7	3.0	•	3.7	•	•
21	010	0.7	3.0	•	3.7	•	•
22	010	0.7	3.0	•	3.7	•	•
23	010	0.7	3.0	•	3.7	•	•
24	010	0.7	3.0	•	3.7	•	•
25	010	0.7	3.0	•	3.7	•	•
26	010	0.7	3.0	•	3.7	•	•
27	010	0.7	3.0	•	3.7	•	•
28	010	0.7	3.0	•	3.7	•	•
29	010	0.7	3.0	•	3.7	•	•
30	010	0.7	3.0	•	3.7	•	•
31	010	0.7	3.0	•	3.7	•	•
32	010	0.7	3.0	•	3.7	•	•
33	010	0.7	3.0	•	3.7	•	•
34	010	0.7	3.0	•	3.7	•	•
35	010	0.7	3.0	•	3.7	•	•
36	010	0.7	3.0	•	3.7	•	•
37	010	0.7	3.0	•	3.7	•	•
38	010	0.7	3.0	•	3.7	•	•
39	010	0.7	3.0	•	3.7	•	•
40	010	0.7	3.0	•	3.7	•	•
41	010	0.7	3.0	•	3.7	•	•
42	010	0.7	3.0	•	3.7	•	•
43	010	0.7	3.0	•	3.7	•	•
44	010	0.7	3.0	•	3.7	•	•
45	010	0.7	3.0	•	3.7	•	•
46	010	0.7	3.0	•	3.7	•	•
47	010	0.7	3.0	•	3.7	•	•
48	010	0.7	3.0	•	3.7	•	•
49	010	0.7	3.0	•	3.7	•	•
50	010	0.7	3.0	•	3.7	•	•
51	010	0.7	3.0	•	3.7	•	•
52	010	0.7	3.0	•	3.7	•	•
53	010	0.7	3.0	•	3.7	•	•
54	010	0.7	3.0	•	3.7	•	•
55	010	0.7	3.0	•	3.7	•	•
56	010	0.7	3.0	•	3.7	•	•
57	010	0.7	3.0	•	3.7	•	•
58	010	0.7	3.0	•	3.7	•	•
59	010	0.7	3.0	•	3.7	•	•
60	010	0.7	3.0	•	3.7	•	•
61	010	0.7	3.0	•	3.7	•	•
62	010	0.7	3.0	•	3.7	•	•
63	010	0.7	3.0	•	3.7	•	•
64	010	0.7	3.0	•	3.7	•	•
65	010	0.7	3.0	•	3.7	•	•
66	010	0.7	3.0	•	3.7	•	•
67	010	0.7	3.0	•	3.7	•	•
68	010	0.7	3.0	•	3.7	•	•
69	010	0.7	3.0	•	3.7	•	•
70	010	0.7	3.0	•	3.7	•	•
71	010	0.7	3.0	•	3.7	•	•
72	010	0.7	3.0	•	3.7	•	•
73	010	0.7	3.0	•	3.7	•	•
74	010	0.7	3.0	•	3.7	•	•
75	010	0.7	3.0	•	3.7	•	•
76	010	0.7	3.0	•	3.7	•	•
77	010	0.7	3.0	•	3.7	•	•
78	010	0.7	3.0	•	3.7	•	•
79	010	0.7	3.0	•	3.7	•	•
80	010	0.7	3.0	•	3.7	•	•
81	010	0.7	3.0	•	3.7	•	•
82	010	0.7	3.0	•	3.7	•	•
83	010	0.7	3.0	•	3.7	•	•
84	010	0.7	3.0	•	3.7	•	•
85	010	0.7	3.0	•	3.7	•	•
86	010	0.7	3.0	•	3.7	•	•
87	010	0.7	3.0	•	3.7	•	•
88	010	0.7	3.0	•	3.7	•	•
89	010	0.7	3.0	•	3.7	•	•
90	010	0.7	3.0	•	3.7	•	•
91	010	0.7	3.0	•	3.7	•	•
92	010	0.7	3.0	•	3.7	•	•
93	010	0.7	3.0	•	3.7	•	•
94	010	0.7	3.0	•	3.7	•	•
95	010	0.7	3.0	•	3.7	•	•
96	010	0.7	3.0	•	3.7	•	•
97	010	0.7	3.0	•	3.7	•	•
98	010	0.7	3.0	•	3.7	•	•
99	010	0.7	3.0	•	3.7	•	•
100	010	0.7	3.0	•	3.7	•	•

Table 10. Results for the Rat Island Earthquake of  
22 November 1965 (additional magnitudes)

100 1.93348 92 0.00000 7.92400 01 MEAN MAGN 4.07  
95 PERCENT CONF. UPPER LIMIT 4.2  
95 PERCENT CONF. LOWER LIMIT 3.9  
SAMPLE VARIANCE 1.0434E 04

1	STATION	2	3	4	5	6	7
			COLP.	CAU	NO.	CAU	
			MG-111		MAG-111		
1	ISL	1.7	6.1	•	4.6	•	•
2	IDL	3.1	6.2	•	6.3	•	•
3	NON	3.3	9.0	•	9.0	•	•
4	MAL	3.3	6.2	•	6.0	•	•
5	VAL	4.3	6.1	•	6.3	•	•
6	PTO	4.3	6.1	•	9.6	•	•
7	HTG	6.7	6.0	•	9.7	•	•
8	ALE	9.9	9.9	•	9.4	•	•
9	HNC	21.9	9.7	•	9.6	•	•
10	NP-17	22.0	9.7	•	9.6	•	•
11	COL	36.3	3.9	•	9.4	•	•
12	MN-18	44.4	6.0	•	6.2	•	•
13	OGD	52.0	6.0	•	6.2	•	•
14	SCP	54.2	6.4	•	6.2	•	•
15	RM-14	54.3	9.6	•	9.6	•	•
16	ULA	58.4	6.0	•	9.0	•	•
17	SJG	60.6	6.1	•	6.3	•	•
18	TRN	61.0	6.1	•	6.0	•	•
19	CPO	63.2	6.0	•	6.4	•	•
20	ATL	64.0	6.0	•	6.4	•	•
21	MV-PA	64.9	9.0	•	9.7	•	•
22	EN-PO	65.2	6.0	•	6.3	•	•
23	SU-PA	65.3	9.6	•	9.5	•	•
24	RO-10	65.3	9.9	•	9.9	•	•
25	OE-11	65.3	6.0	•	6.4	•	•
26	UN-10	65.4	9.9	•	6.3	•	•
27	CAB	65.6	6.1	•	6.0	•	•
28	HC-PO	65.7	9.6	•	6.3	•	•
29	CR-18	65.8	9.9	•	6.3	•	•
30	RCD	66.3	9.6	•	6.5	•	•
31	OOT	66.3	9.6	•	6.0	•	•
32	OSC	69.3	9.0	•	9.6	•	•
33	SPO	69.4	9.6	•	4.2	•	•
34	GV-17	72.6	6.0	•	9.6	•	•
35	OMO	73.6	9.6	•	9.1	•	•
36	UHO	74.2	9.6	•	6.1	•	•
37	LUM	75.3	6.0	•	9.6	•	•
38	OUG	76.2	9.9	•	9.6	•	•
39	COR	77.5	9.0	•	9.7	•	•
40	EUR	78.2	9.6	•	9.6	•	•
41	KN-17	79.5	9.6	•	9.7	•	•
42	TFO	81.4	9.6	•	9.3	•	•
43	TUC	82.9	9.6	•	9.3	•	•
44	ONS	85.4	9.6	•	4.0	•	•
45	RIV	203.4	6.1	•	9.6	•	•
46	CTA	212.6	6.1	•	9.4	•	•
47	DAV	244.9	6.1	•	9.6	•	•
48	LEM	251.7	6.2	•	9.7	•	•
49	HAN	254.1	6.1	•	9.5	•	•
50	GAG	256.3	6.2	•	9.4	•	•
51	HNC	265.7	6.2	•	6.0	•	•
52	SEO	270.5	6.2	•	9.0	•	•
53	SML	265.4	6.2	•	6.4	•	•
54	RND	285.6	6.2	•	9.7	•	•
55	PNO	284.0	6.2	•	6.3	•	•
56	NOI	267.9	6.2	•	6.1	•	•
57	LAM	301.4	6.2	•	6.6	•	•
58	QUE	305.7	6.2	•	6.1	•	•
59	SMI	316.9	6.2	•	6.1	•	•
60	JEN	330.7	6.2	•	9.3	•	•
61	AUR	347.1	6.1	•	6.4	•	•
62	HEV	349.1	6.1	•	9.0	•	•
63	TOI	350.1	6.2	•	9.7	•	•
64	POI	352.6	6.2	•	6.1	•	•
65	COP	352.6	6.1	•	6.4	•	•
66	STU	353.9	6.2	•	9.6	•	•
67	KON	354.9	6.1	•	6.3	•	•
68	IFW	4.4	6.2	•	0	•	•
69	HNG	54.4	6.0	•	0	•	•
70	ADM	56.8	6.0	•	0	•	•
71	SJP	60.6	6.1	•	0	•	•
72	DEF	64.3	6.0	•	0	•	•
73	SMA	64.2	6.0	•	0	•	•
74	TCO	404.9	6.1	•	0	•	•
75	MAB	412.6	9.9	•	0	•	•
76	PWG	415.4	6.0	•	0	•	•
77	ANP	467.1	6.2	•	0	•	•
78	QMA	262.6	6.2	•	0	•	•
79	PEO	465.2	6.2	•	0	•	•
80	CHG	275.3	6.2	•	0	•	•
81	WON	285.6	6.2	•	0	•	•
82	QNH	314.6	9.2	•	0	•	•
83	TAB	320.6	6.2	•	0	•	•
84	UNC	334.2	6.2	•	0	•	•
85	IST	338.5	6.2	•	0	•	•
86	ETH	341.6	6.2	•	0	•	•
87	PRI	350.9	6.2	•	0	•	•
88	HNC	351.1	6.2	•	0	•	•

Table 11. Results for the Hindu Kush Earthquake of 28 January 1964.

1.6000E 03 CONVA 6.0612E 02 MEAN MAG= 6.39  
 95 PERCENT CONF. UPPER LIMIT 6.5  
 95 PERCENT CONF. LOWER LIMIT 6.3  
 SAMPLE VARIANCE= 2.1128E 05

I	STATION	AZIMUTH	CALC.		OBS.	
			HA (1)	HA (2)	MAG (1)	MAG (2)
1	PHO	0	6.4	*	6.3	*
2	MOZ	1.0	6.4	*	6.1	*
3	NP-	3.0	6.4	*	6.1	*
4	MMH	6.0	6.4	*	5.6	*
5	LON	9.0	6.3	*	6.2	*
6	MTJ	10.0	6.1	-	6.1	*
7	AMU	71.0	6.1	-	6.1	*
8	ANP	90.0	5.9	-	6.5	-
9	HAG	103.0	5.4	-	5.9	-
10	PHG	106.0	4.5	-	6.1	-
11	NWA	135.0	5.6	*	5.4	-
12	CHI	295.0	6.6	*	7.0	*
13	LIS	299.0	6.6	*	7.2	*
14	LJU	301.0	6.7	*	6.4	*
15	PSZ	303.0	6.7	*	7.0	*
16	VIE	304.0	6.7	*	6.7	*
17	STU	306.0	6.7	*	5.9	*
18	PHU	307.0	6.7	*	6.5	*
19	MOX	308.0	6.7	*	7.0	*
20	MNS	309.0	6.7	*	6.3	*
21	WAW	330.0	6.8	*	7.2	*
22	KEM	331.0	6.7	*	6.5	*
23	COP	335.0	6.8	*	6.9	*
24	NUH	334.0	6.4	*	7.0	*
25	KTG	336.0	6.7	*	6.4	*
26	BLA	337.0	6.5	*	5.5	*
27	KEV	338.0	6.7	*	6.6	*
28	NUH	350.0	6.6	*	6.2	*
29	WCD	356.0	6.4	*	6.7	*
30	MNR	98.1	4.1	-	0	-
31	NAH	98.5	4.9	-	0	-
32	MKC	98.5	5.6	-	0	-
33	SHL	135.4	6.1	*	0	-
34	CHG	138.0	5.9	*	0	-
35	MUN	142.2	5.3	-	0	*
36	NDI	143.9	6.0	*	0	-
37	QUE	204.0	6.0	*	0	-
38	PRE	219.0	6.3	-	0	*
39	HUL	222.6	6.3	-	0	*
40	NAI	227.0	6.5	-	0	*
41	WIN	229.8	6.1	-	0	*
42	AAE	234.9	6.5	-	0	*
43	SHI	250.9	6.0	*	0	*
44	HLW	270.3	6.1	*	0	*
45	ATU	286.9	6.6	*	0	*
46	IST	291.0	6.6	*	0	*
47	MAL	294.0	6.6	*	0	*
48	AQU	296.0	6.7	*	0	*
49	TOL	298.1	6.6	*	0	*
50	PTJ	301.0	6.6	*	0	*
51	PIA	304.7	6.6	*	0	*
52	VIN	313.3	6.7	*	0	*
53	KOH	321.0	6.8	*	0	*

Table 12. Results for the Alaskan Earthquake of 28 March 1964.

1. 1.30:00 US L14440 1.12770 00 0000 0000 7.30  
 00 000000 0000 0000 0000 0000  
 00 000000 0000 0000 0000 0000  
 0000 000000 0.0000 00

1	STATION	AMPL	PER	CM	CM	CM
1	V16	11.0	0.0	0.0	0.0	0.0
2	V17	11.0	0.0	0.0	0.0	0.0
3	V18	11.0	0.0	0.0	0.0	0.0
4	V19	11.0	0.0	0.0	0.0	0.0
5	V20	11.0	0.0	0.0	0.0	0.0
6	V21	11.0	0.0	0.0	0.0	0.0
7	V22	11.0	0.0	0.0	0.0	0.0
8	V23	11.0	0.0	0.0	0.0	0.0
9	V24	11.0	0.0	0.0	0.0	0.0
10	V25	11.0	0.0	0.0	0.0	0.0
11	V26	11.0	0.0	0.0	0.0	0.0
12	V27	11.0	0.0	0.0	0.0	0.0
13	V28	11.0	0.0	0.0	0.0	0.0
14	V29	11.0	0.0	0.0	0.0	0.0
15	V30	11.0	0.0	0.0	0.0	0.0
16	V31	11.0	0.0	0.0	0.0	0.0
17	V32	11.0	0.0	0.0	0.0	0.0
18	V33	11.0	0.0	0.0	0.0	0.0
19	V34	11.0	0.0	0.0	0.0	0.0
20	V35	11.0	0.0	0.0	0.0	0.0
21	V36	11.0	0.0	0.0	0.0	0.0
22	V37	11.0	0.0	0.0	0.0	0.0
23	V38	11.0	0.0	0.0	0.0	0.0
24	V39	11.0	0.0	0.0	0.0	0.0
25	V40	11.0	0.0	0.0	0.0	0.0
26	V41	11.0	0.0	0.0	0.0	0.0
27	V42	11.0	0.0	0.0	0.0	0.0
28	V43	11.0	0.0	0.0	0.0	0.0
29	V44	11.0	0.0	0.0	0.0	0.0
30	V45	11.0	0.0	0.0	0.0	0.0
31	V46	11.0	0.0	0.0	0.0	0.0
32	V47	11.0	0.0	0.0	0.0	0.0
33	V48	11.0	0.0	0.0	0.0	0.0
34	V49	11.0	0.0	0.0	0.0	0.0
35	V50	11.0	0.0	0.0	0.0	0.0
36	V51	11.0	0.0	0.0	0.0	0.0
37	V52	11.0	0.0	0.0	0.0	0.0
38	V53	11.0	0.0	0.0	0.0	0.0
39	V54	11.0	0.0	0.0	0.0	0.0
40	V55	11.0	0.0	0.0	0.0	0.0
41	V56	11.0	0.0	0.0	0.0	0.0
42	V57	11.0	0.0	0.0	0.0	0.0
43	V58	11.0	0.0	0.0	0.0	0.0
44	V59	11.0	0.0	0.0	0.0	0.0
45	V60	11.0	0.0	0.0	0.0	0.0
46	V61	11.0	0.0	0.0	0.0	0.0
47	V62	11.0	0.0	0.0	0.0	0.0
48	V63	11.0	0.0	0.0	0.0	0.0
49	V64	11.0	0.0	0.0	0.0	0.0
50	V65	11.0	0.0	0.0	0.0	0.0
51	V66	11.0	0.0	0.0	0.0	0.0
52	V67	11.0	0.0	0.0	0.0	0.0
53	V68	11.0	0.0	0.0	0.0	0.0
54	V69	11.0	0.0	0.0	0.0	0.0
55	V70	11.0	0.0	0.0	0.0	0.0
56	V71	11.0	0.0	0.0	0.0	0.0
57	V72	11.0	0.0	0.0	0.0	0.0
58	V73	11.0	0.0	0.0	0.0	0.0
59	V74	11.0	0.0	0.0	0.0	0.0
60	V75	11.0	0.0	0.0	0.0	0.0
61	V76	11.0	0.0	0.0	0.0	0.0
62	V77	11.0	0.0	0.0	0.0	0.0
63	V78	11.0	0.0	0.0	0.0	0.0
64	V79	11.0	0.0	0.0	0.0	0.0
65	V80	11.0	0.0	0.0	0.0	0.0
66	V81	11.0	0.0	0.0	0.0	0.0
67	V82	11.0	0.0	0.0	0.0	0.0
68	V83	11.0	0.0	0.0	0.0	0.0
69	V84	11.0	0.0	0.0	0.0	0.0
70	V85	11.0	0.0	0.0	0.0	0.0
71	V86	11.0	0.0	0.0	0.0	0.0
72	V87	11.0	0.0	0.0	0.0	0.0
73	V88	11.0	0.0	0.0	0.0	0.0
74	V89	11.0	0.0	0.0	0.0	0.0
75	V90	11.0	0.0	0.0	0.0	0.0
76	V91	11.0	0.0	0.0	0.0	0.0
77	V92	11.0	0.0	0.0	0.0	0.0
78	V93	11.0	0.0	0.0	0.0	0.0
79	V94	11.0	0.0	0.0	0.0	0.0
80	V95	11.0	0.0	0.0	0.0	0.0
81	V96	11.0	0.0	0.0	0.0	0.0
82	V97	11.0	0.0	0.0	0.0	0.0
83	V98	11.0	0.0	0.0	0.0	0.0
84	V99	11.0	0.0	0.0	0.0	0.0
85	V100	11.0	0.0	0.0	0.0	0.0



Table 13. Results for the Alaskan Earthquake of  
28 March 1964 (additional first motions).

Station	Time	Phase	Amplitude	Period	Direction
100	00.0	P	0.0	0.0	0.0
101	00.0	P	0.0	0.0	0.0
102	00.0	P	0.0	0.0	0.0
103	00.0	P	0.0	0.0	0.0
104	00.0	P	0.0	0.0	0.0
105	00.0	P	0.0	0.0	0.0
106	00.0	P	0.0	0.0	0.0
107	00.0	P	0.0	0.0	0.0
108	00.0	P	0.0	0.0	0.0
109	00.0	P	0.0	0.0	0.0
110	00.0	P	0.0	0.0	0.0
111	00.0	P	0.0	0.0	0.0
112	00.0	P	0.0	0.0	0.0
113	00.0	P	0.0	0.0	0.0
114	00.0	P	0.0	0.0	0.0
115	00.0	P	0.0	0.0	0.0
116	00.0	P	0.0	0.0	0.0
117	00.0	P	0.0	0.0	0.0
118	00.0	P	0.0	0.0	0.0
119	00.0	P	0.0	0.0	0.0
120	00.0	P	0.0	0.0	0.0
121	00.0	P	0.0	0.0	0.0
122	00.0	P	0.0	0.0	0.0
123	00.0	P	0.0	0.0	0.0
124	00.0	P	0.0	0.0	0.0
125	00.0	P	0.0	0.0	0.0
126	00.0	P	0.0	0.0	0.0
127	00.0	P	0.0	0.0	0.0
128	00.0	P	0.0	0.0	0.0
129	00.0	P	0.0	0.0	0.0
130	00.0	P	0.0	0.0	0.0
131	00.0	P	0.0	0.0	0.0
132	00.0	P	0.0	0.0	0.0
133	00.0	P	0.0	0.0	0.0
134	00.0	P	0.0	0.0	0.0
135	00.0	P	0.0	0.0	0.0
136	00.0	P	0.0	0.0	0.0
137	00.0	P	0.0	0.0	0.0
138	00.0	P	0.0	0.0	0.0
139	00.0	P	0.0	0.0	0.0
140	00.0	P	0.0	0.0	0.0
141	00.0	P	0.0	0.0	0.0
142	00.0	P	0.0	0.0	0.0
143	00.0	P	0.0	0.0	0.0
144	00.0	P	0.0	0.0	0.0
145	00.0	P	0.0	0.0	0.0
146	00.0	P	0.0	0.0	0.0
147	00.0	P	0.0	0.0	0.0
148	00.0	P	0.0	0.0	0.0
149	00.0	P	0.0	0.0	0.0
150	00.0	P	0.0	0.0	0.0
151	00.0	P	0.0	0.0	0.0
152	00.0	P	0.0	0.0	0.0
153	00.0	P	0.0	0.0	0.0
154	00.0	P	0.0	0.0	0.0
155	00.0	P	0.0	0.0	0.0
156	00.0	P	0.0	0.0	0.0
157	00.0	P	0.0	0.0	0.0
158	00.0	P	0.0	0.0	0.0
159	00.0	P	0.0	0.0	0.0
160	00.0	P	0.0	0.0	0.0
161	00.0	P	0.0	0.0	0.0
162	00.0	P	0.0	0.0	0.0
163	00.0	P	0.0	0.0	0.0
164	00.0	P	0.0	0.0	0.0
165	00.0	P	0.0	0.0	0.0
166	00.0	P	0.0	0.0	0.0
167	00.0	P	0.0	0.0	0.0
168	00.0	P	0.0	0.0	0.0
169	00.0	P	0.0	0.0	0.0
170	00.0	P	0.0	0.0	0.0
171	00.0	P	0.0	0.0	0.0
172	00.0	P	0.0	0.0	0.0
173	00.0	P	0.0	0.0	0.0
174	00.0	P	0.0	0.0	0.0
175	00.0	P	0.0	0.0	0.0
176	00.0	P	0.0	0.0	0.0
177	00.0	P	0.0	0.0	0.0
178	00.0	P	0.0	0.0	0.0
179	00.0	P	0.0	0.0	0.0
180	00.0	P	0.0	0.0	0.0
181	00.0	P	0.0	0.0	0.0
182	00.0	P	0.0	0.0	0.0
183	00.0	P	0.0	0.0	0.0
184	00.0	P	0.0	0.0	0.0
185	00.0	P	0.0	0.0	0.0
186	00.0	P	0.0	0.0	0.0
187	00.0	P	0.0	0.0	0.0
188	00.0	P	0.0	0.0	0.0
189	00.0	P	0.0	0.0	0.0
190	00.0	P	0.0	0.0	0.0
191	00.0	P	0.0	0.0	0.0
192	00.0	P	0.0	0.0	0.0
193	00.0	P	0.0	0.0	0.0
194	00.0	P	0.0	0.0	0.0
195	00.0	P	0.0	0.0	0.0
196	00.0	P	0.0	0.0	0.0
197	00.0	P	0.0	0.0	0.0
198	00.0	P	0.0	0.0	0.0
199	00.0	P	0.0	0.0	0.0
200	00.0	P	0.0	0.0	0.0

**Table 14. Results for the Niigata Earthquake of 16 June 1964.**

NO	DESCRIPTION	QTY	UNIT	PRICE	TOTAL	TAX	NET
01	CLB	25.00	EA	0.7	17.50	0.00	17.50
02	COB	35.00	EA	0.7	24.50	0.00	24.50
03	CPB	35.00	EA	0.7	24.50	0.00	24.50
04	DBB	40.00	EA	0.7	28.00	0.00	28.00
05	DOB	40.00	EA	0.7	28.00	0.00	28.00
06	EOB	40.00	EA	0.7	28.00	0.00	28.00
07	FOB	40.00	EA	0.7	28.00	0.00	28.00
08	GFB	40.00	EA	0.7	28.00	0.00	28.00
09	HOB	40.00	EA	0.7	28.00	0.00	28.00
10	IOB	40.00	EA	0.7	28.00	0.00	28.00
11	POB	40.00	EA	0.7	28.00	0.00	28.00
12	QOB	40.00	EA	0.7	28.00	0.00	28.00
13	ROB	40.00	EA	0.7	28.00	0.00	28.00
14	SOB	40.00	EA	0.7	28.00	0.00	28.00
15	TOB	40.00	EA	0.7	28.00	0.00	28.00
16	UOB	40.00	EA	0.7	28.00	0.00	28.00
17	VOB	40.00	EA	0.7	28.00	0.00	28.00
18	WOB	40.00	EA	0.7	28.00	0.00	28.00
19	XOB	40.00	EA	0.7	28.00	0.00	28.00
20	YOB	40.00	EA	0.7	28.00	0.00	28.00
21	ZOB	40.00	EA	0.7	28.00	0.00	28.00
22	AOB	40.00	EA	0.7	28.00	0.00	28.00
23	BOB	40.00	EA	0.7	28.00	0.00	28.00
24	COB	40.00	EA	0.7	28.00	0.00	28.00
25	DOB	40.00	EA	0.7	28.00	0.00	28.00
26	EOB	40.00	EA	0.7	28.00	0.00	28.00
27	FOB	40.00	EA	0.7	28.00	0.00	28.00
28	GFB	40.00	EA	0.7	28.00	0.00	28.00
29	HOB	40.00	EA	0.7	28.00	0.00	28.00
30	IOB	40.00	EA	0.7	28.00	0.00	28.00
31	POB	40.00	EA	0.7	28.00	0.00	28.00
32	QOB	40.00	EA	0.7	28.00	0.00	28.00
33	ROB	40.00	EA	0.7	28.00	0.00	28.00
34	SOB	40.00	EA	0.7	28.00	0.00	28.00
35	TOB	40.00	EA	0.7	28.00	0.00	28.00
36	UOB	40.00	EA	0.7	28.00	0.00	28.00
37	VOB	40.00	EA	0.7	28.00	0.00	28.00
38	WOB	40.00	EA	0.7	28.00	0.00	28.00
39	XOB	40.00	EA	0.7	28.00	0.00	28.00
40	YOB	40.00	EA	0.7	28.00	0.00	28.00
41	ZOB	40.00	EA	0.7	28.00	0.00	28.00
42	AOB	40.00	EA	0.7	28.00	0.00	28.00
43	BOB	40.00	EA	0.7	28.00	0.00	28.00
44	COB	40.00	EA	0.7	28.00	0.00	28.00
45	DOB	40.00	EA	0.7	28.00	0.00	28.00
46	EOB	40.00	EA	0.7	28.00	0.00	28.00
47	FOB	40.00	EA	0.7	28.00	0.00	28.00
48	GFB	40.00	EA	0.7	28.00	0.00	28.00
49	HOB	40.00	EA	0.7	28.00	0.00	28.00
50	IOB	40.00	EA	0.7	28.00	0.00	28.00
51	POB	40.00	EA	0.7	28.00	0.00	28.00
52	QOB	40.00	EA	0.7	28.00	0.00	28.00
53	ROB	40.00	EA	0.7	28.00	0.00	28.00
54	SOB	40.00	EA	0.7	28.00	0.00	28.00
55	TOB	40.00	EA	0.7	28.00	0.00	28.00
56	UOB	40.00	EA	0.7	28.00	0.00	28.00

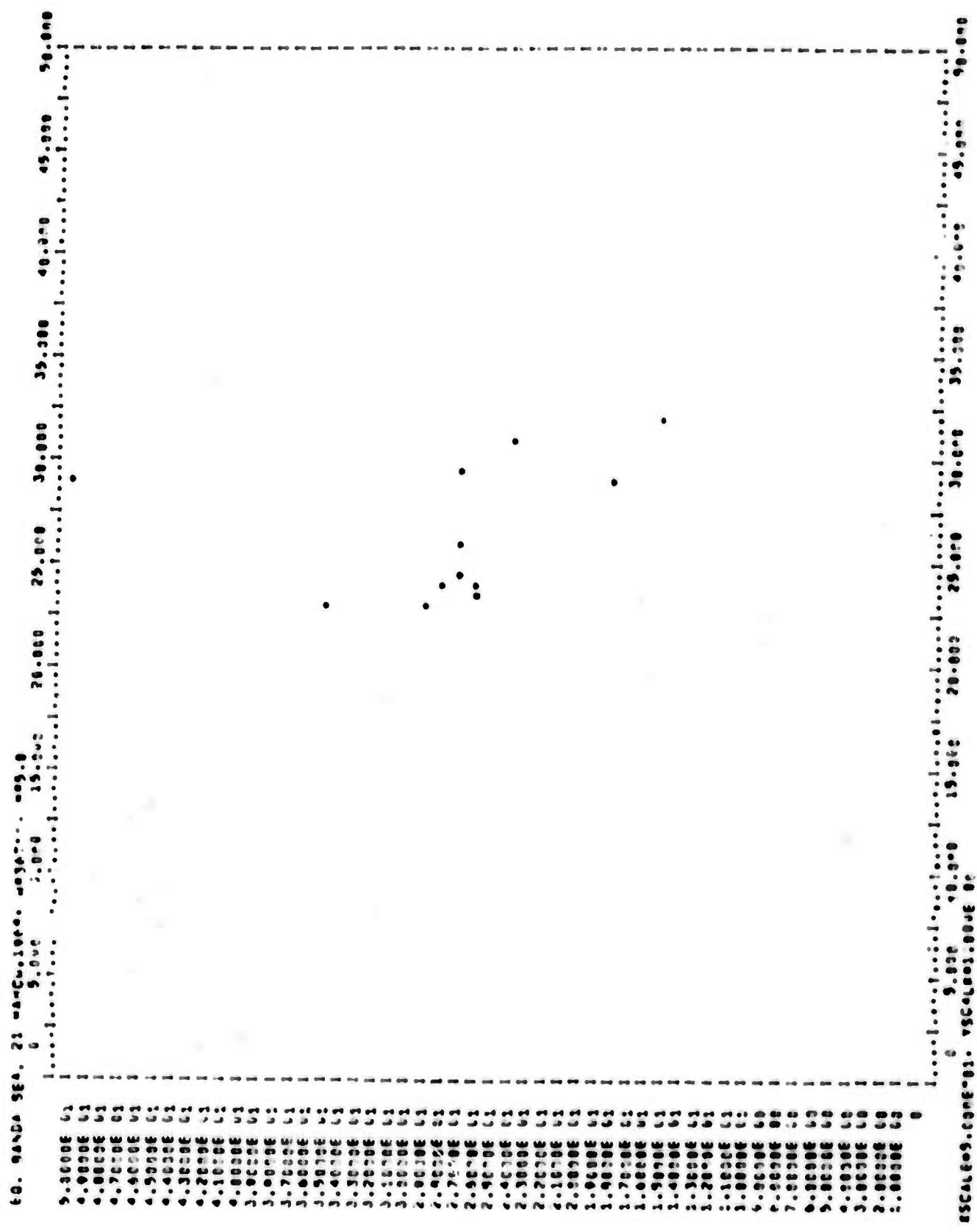


Figure 1. Observed Radiation Pattern for the Banda Sea Earthquake of 21 March 1964.



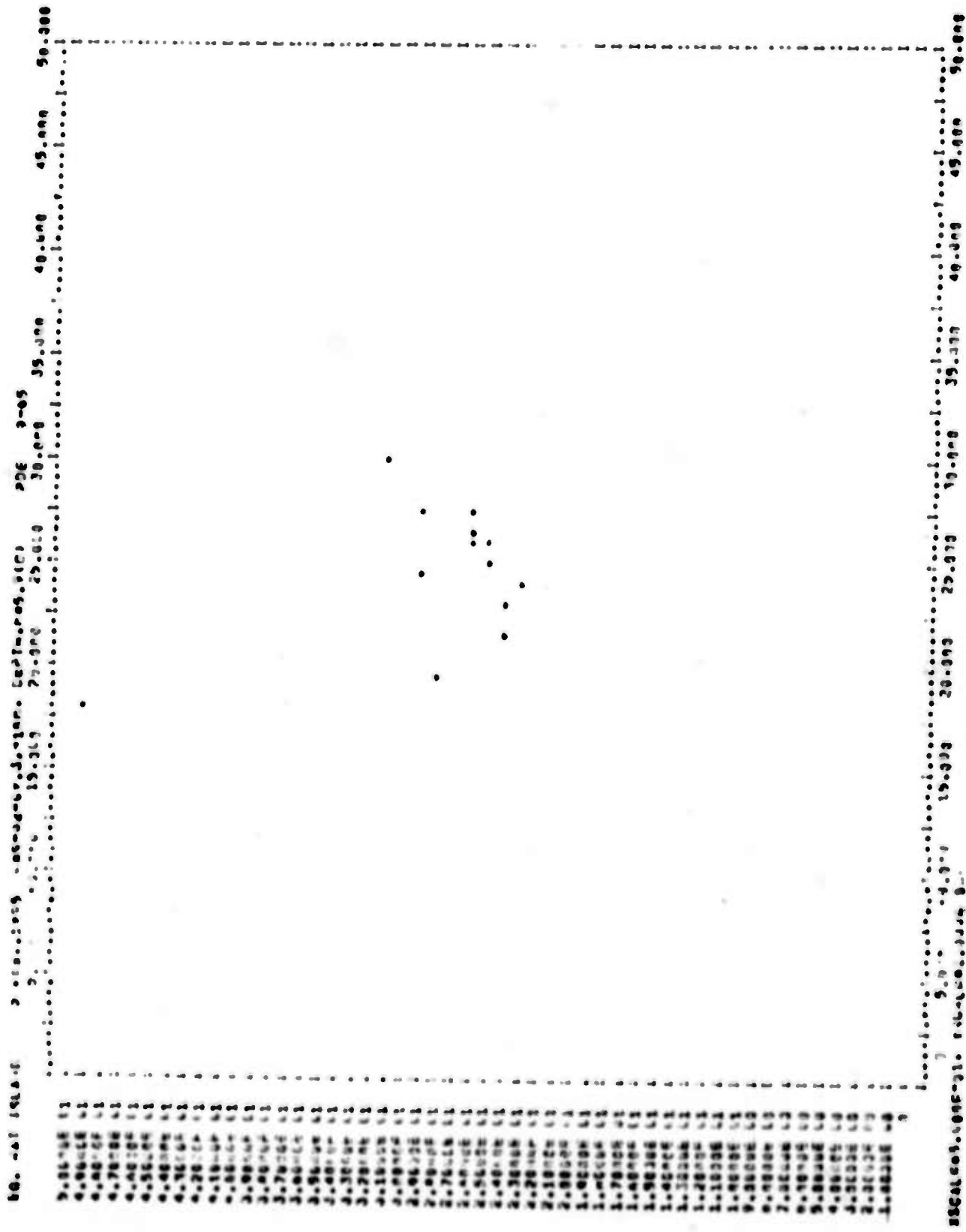


Figure 3. Observed Radiation Pattern for the Rat Island Earthquake of 5 February 1965.





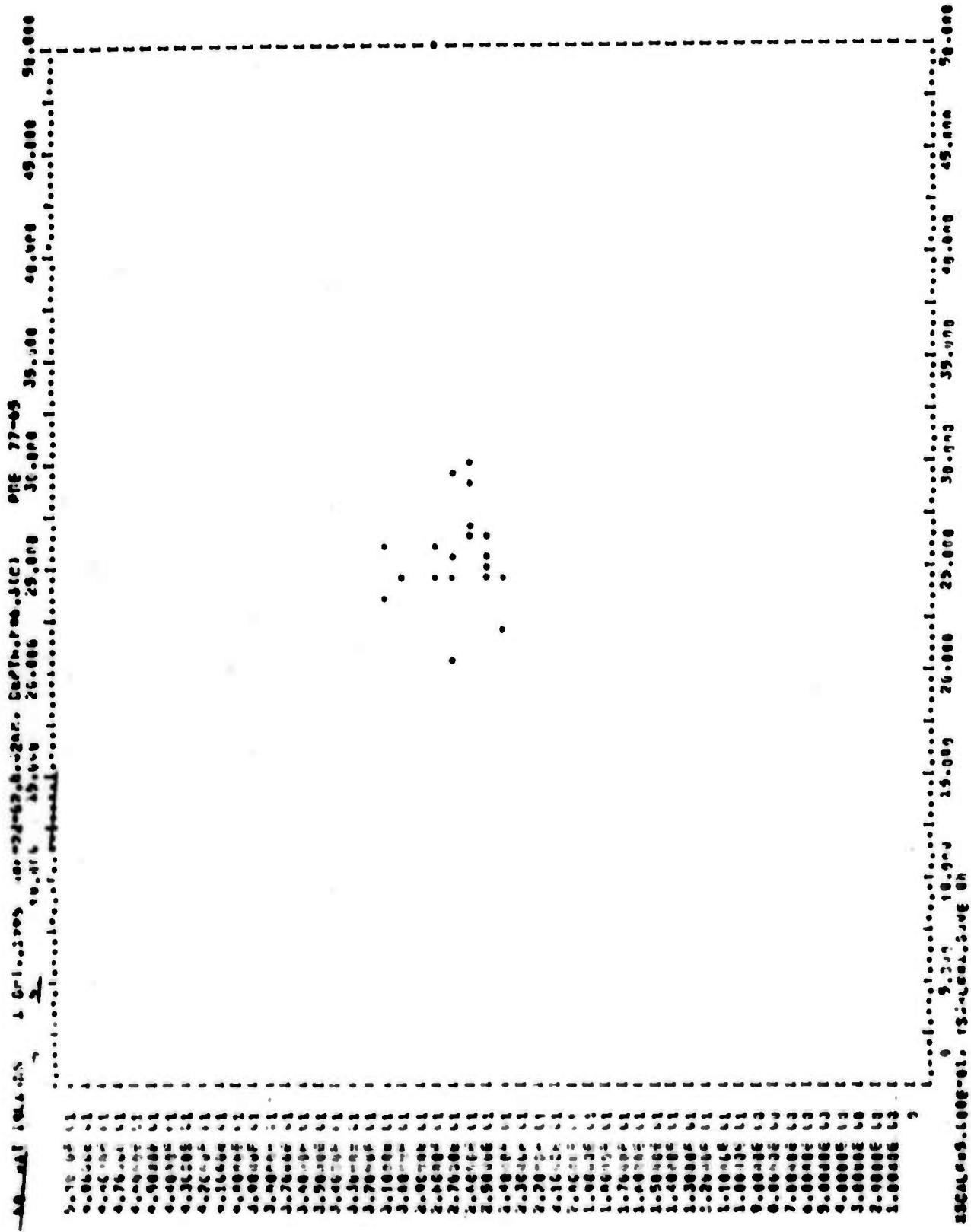


Figure 5. Observed Radiation Pattern for the Rat Island Earthquake of 1 October 1965.

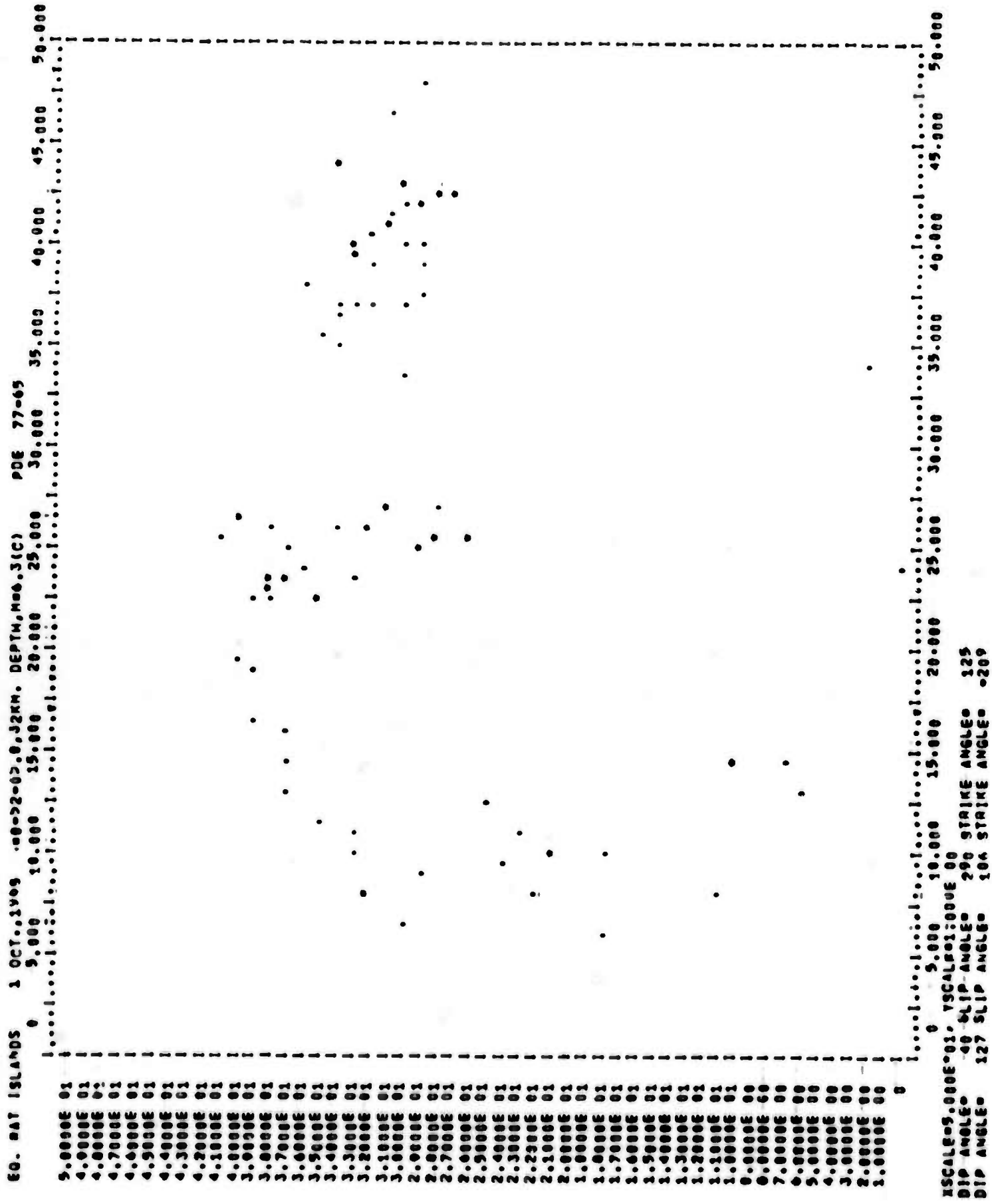


Figure 6. Calculated Radiation Pattern for the Rat Island Earthquake of 1 October 1965.

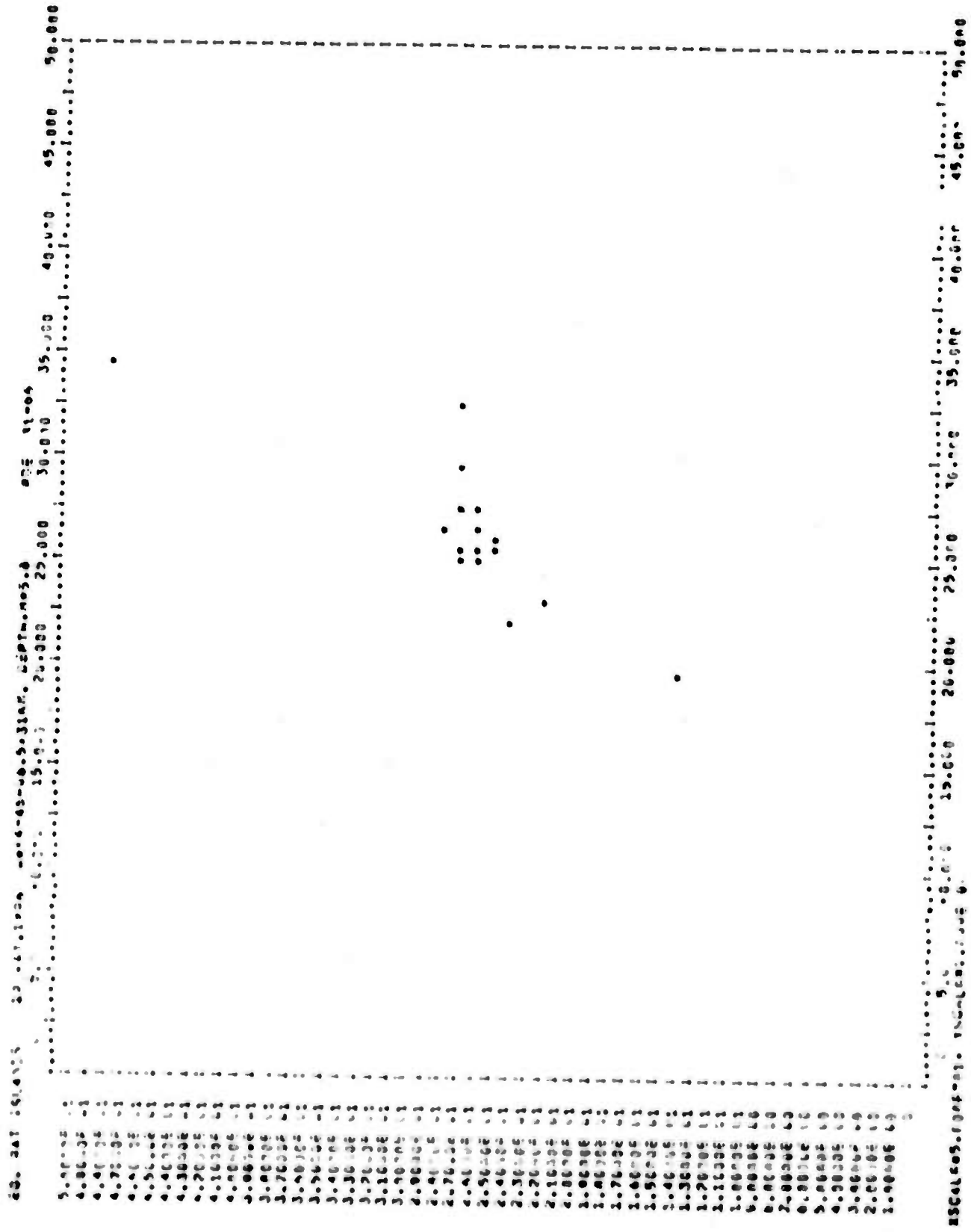


Figure 7. Observed Radiation Pattern for the Rat Island Earthquake of 15 May 1966.





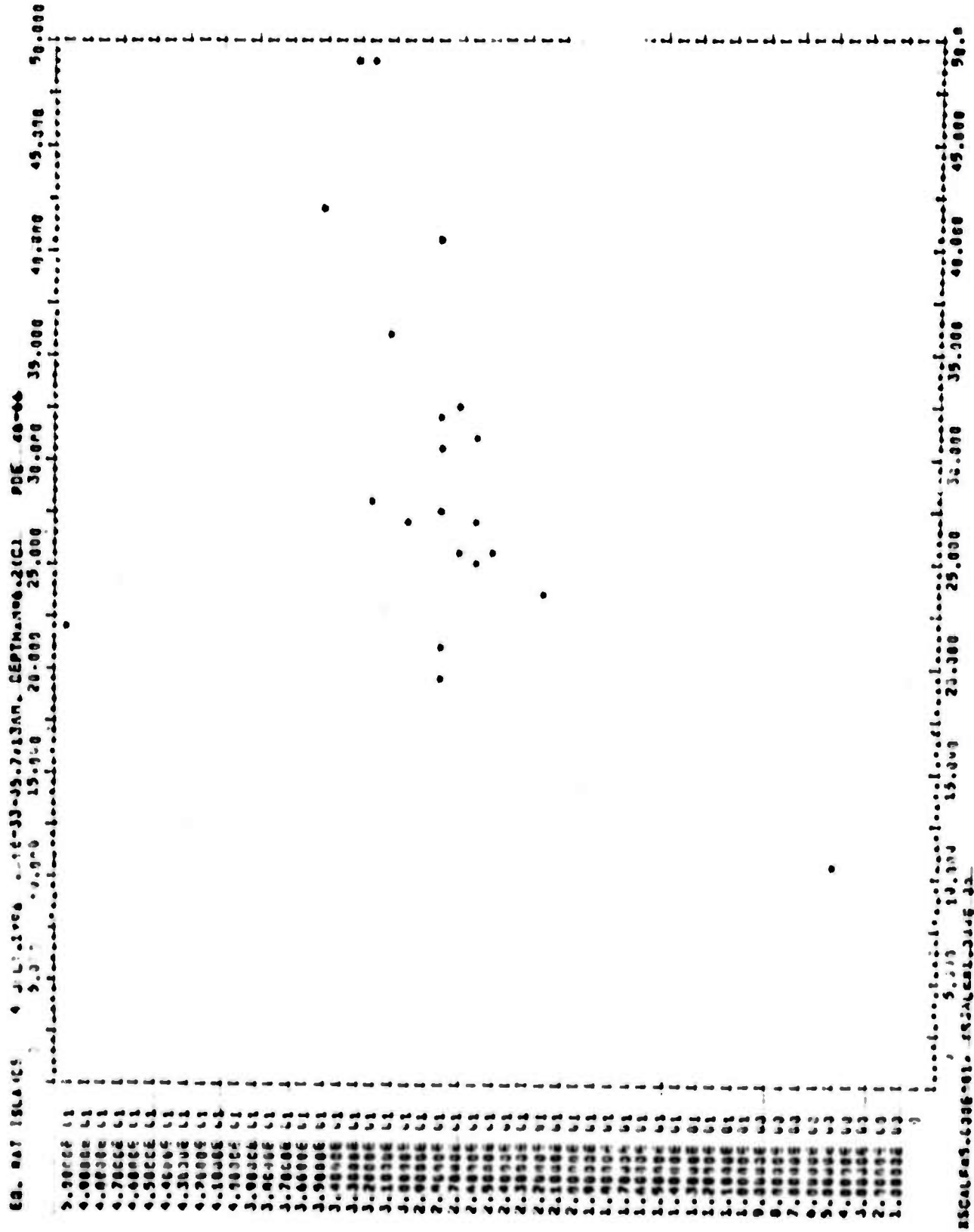


Figure 9. Observed Radiation Pattern for the Rat Island Earthquake of 4 July 1966.



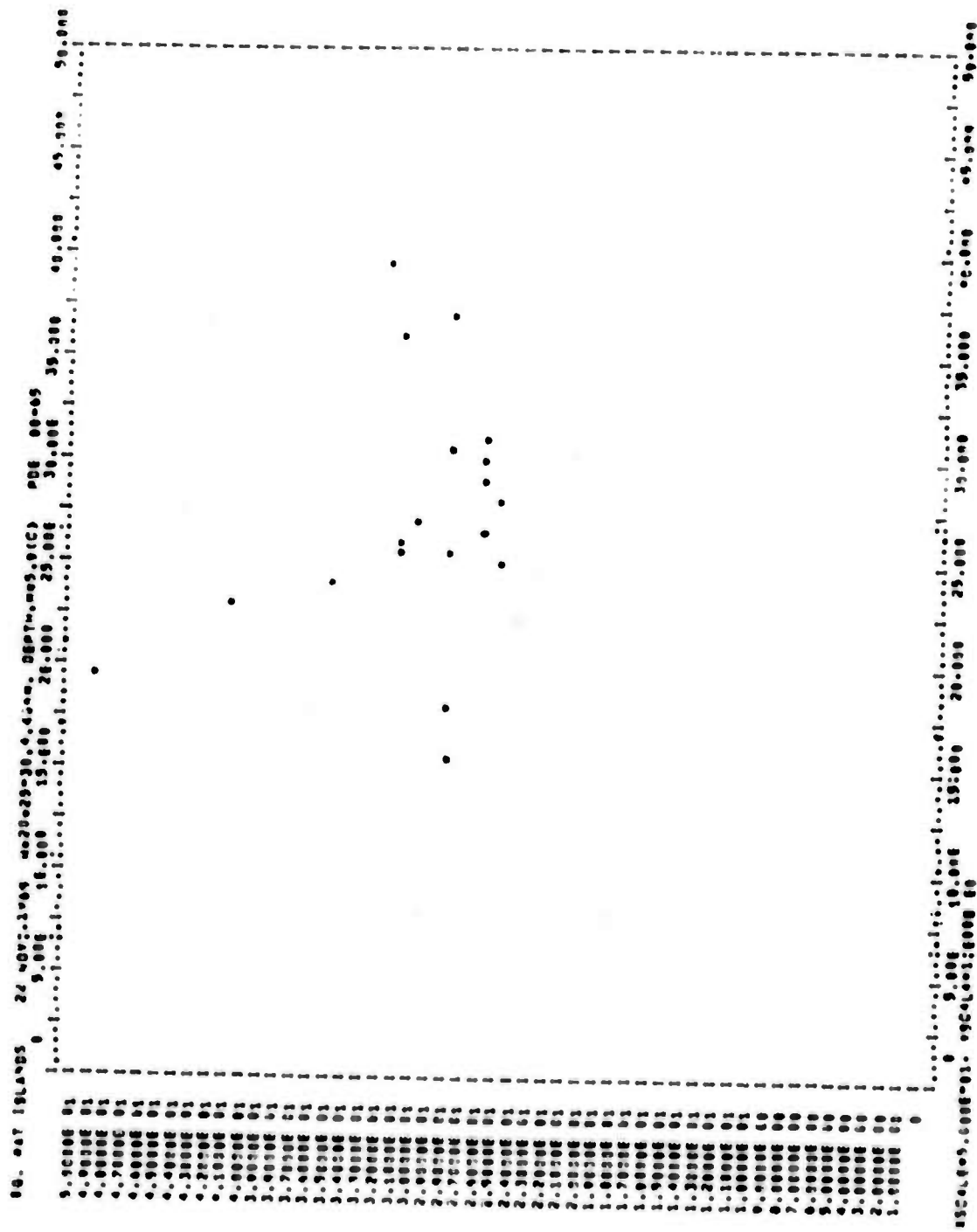


Figure 11. Observed Radiation Pattern for the Rat Island Earthquake of 22 November 1965.



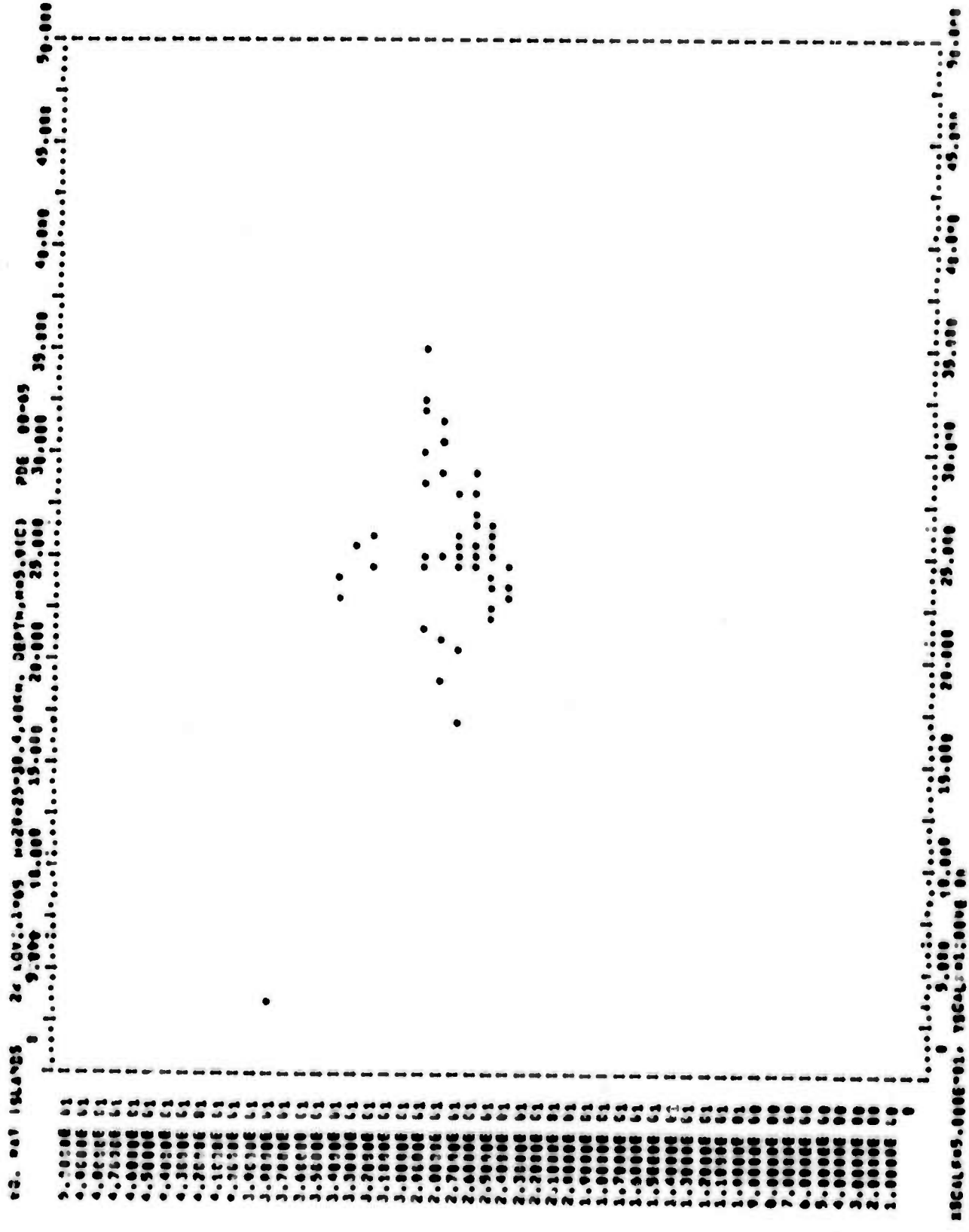


Figure 13. Observed Radiation Pattern for the Rat Island Earthquake of 22 November 1965 (additional magnitudes).



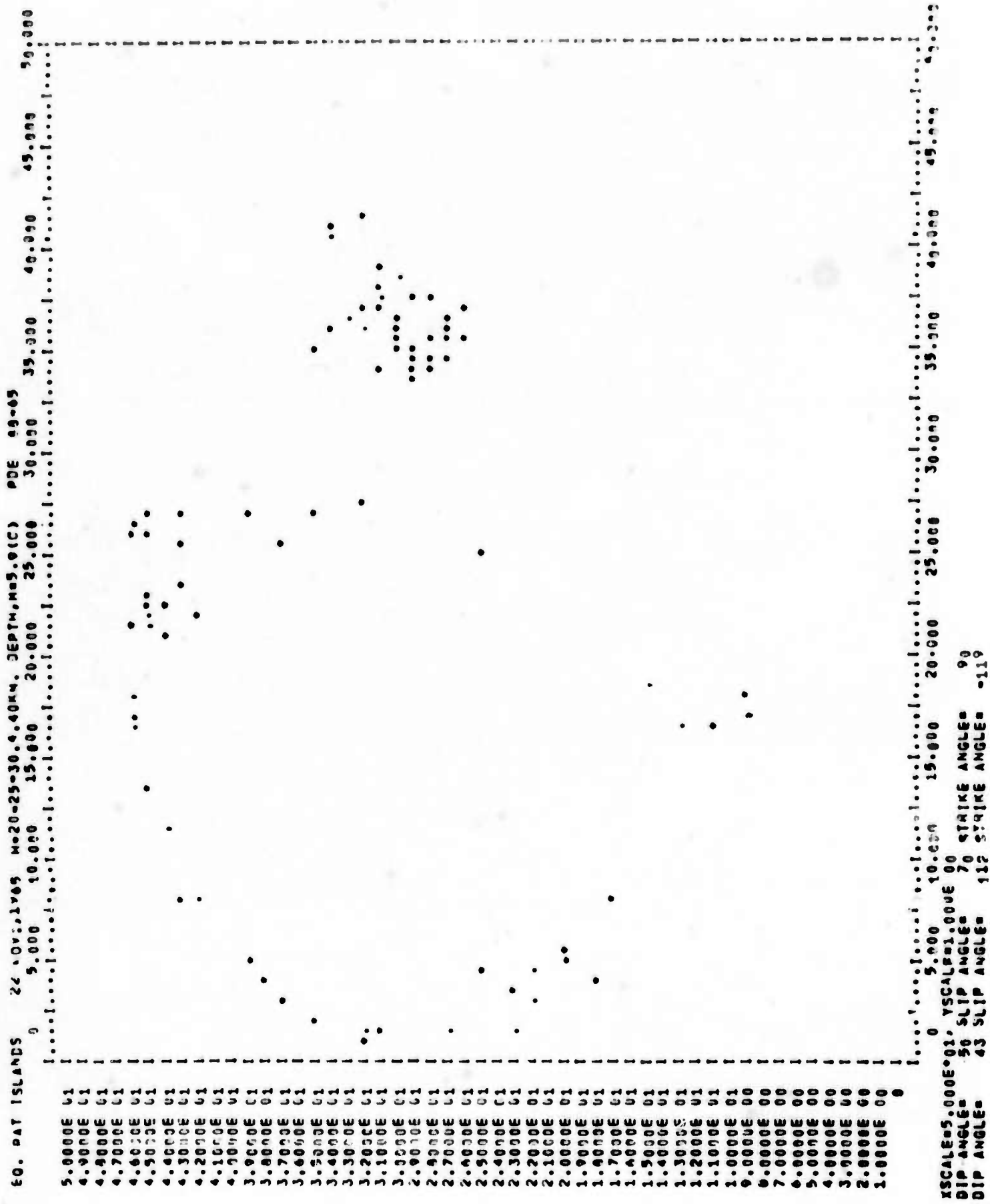


Figure 14. Calculated Radiation Pattern for the Rat Island Earthquake of 22 November 1965 (additional magnitudes).



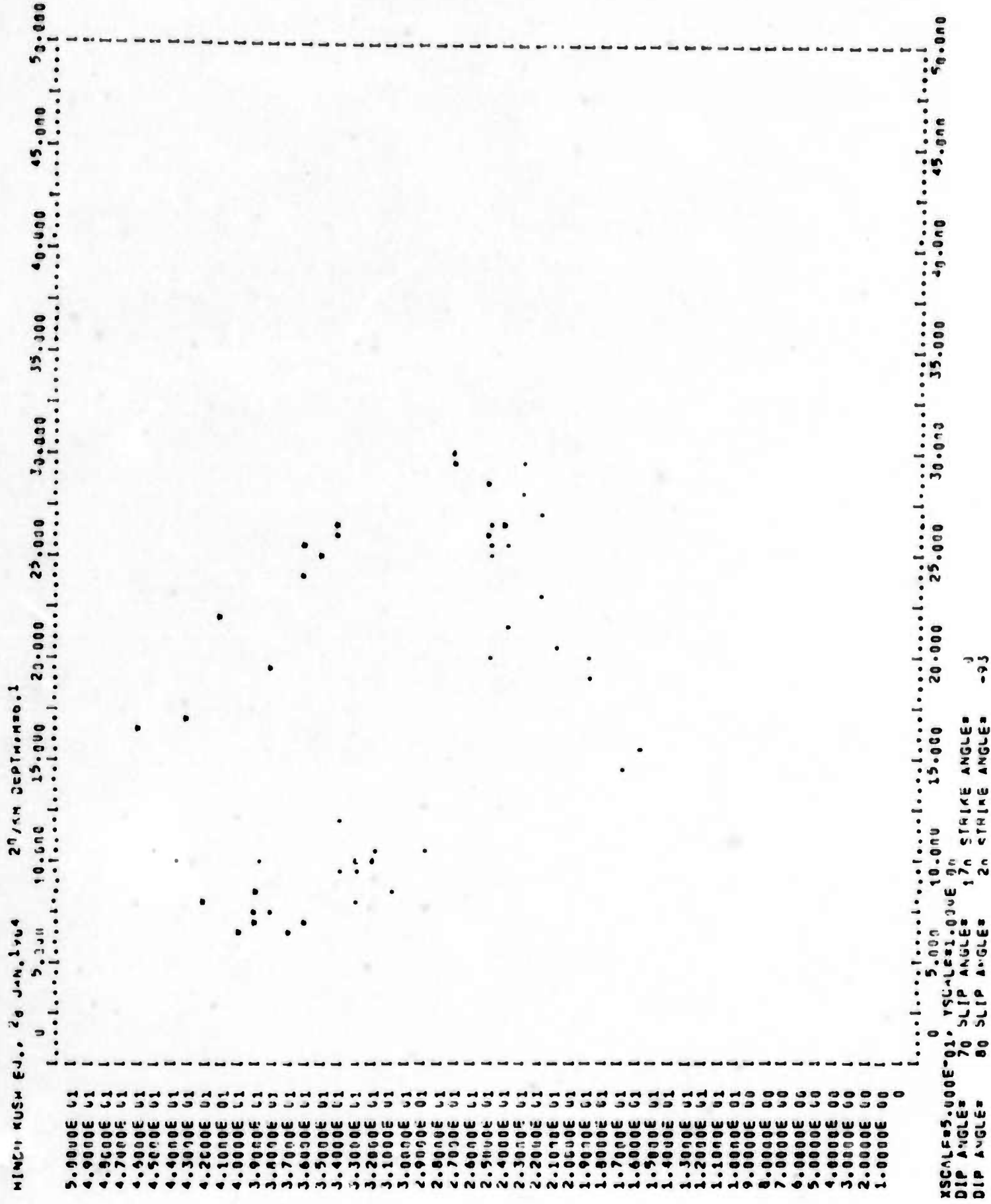


Figure 16. Calculated Radiation Pattern for the Hindu Kush Earthquake of 28 January 1964.

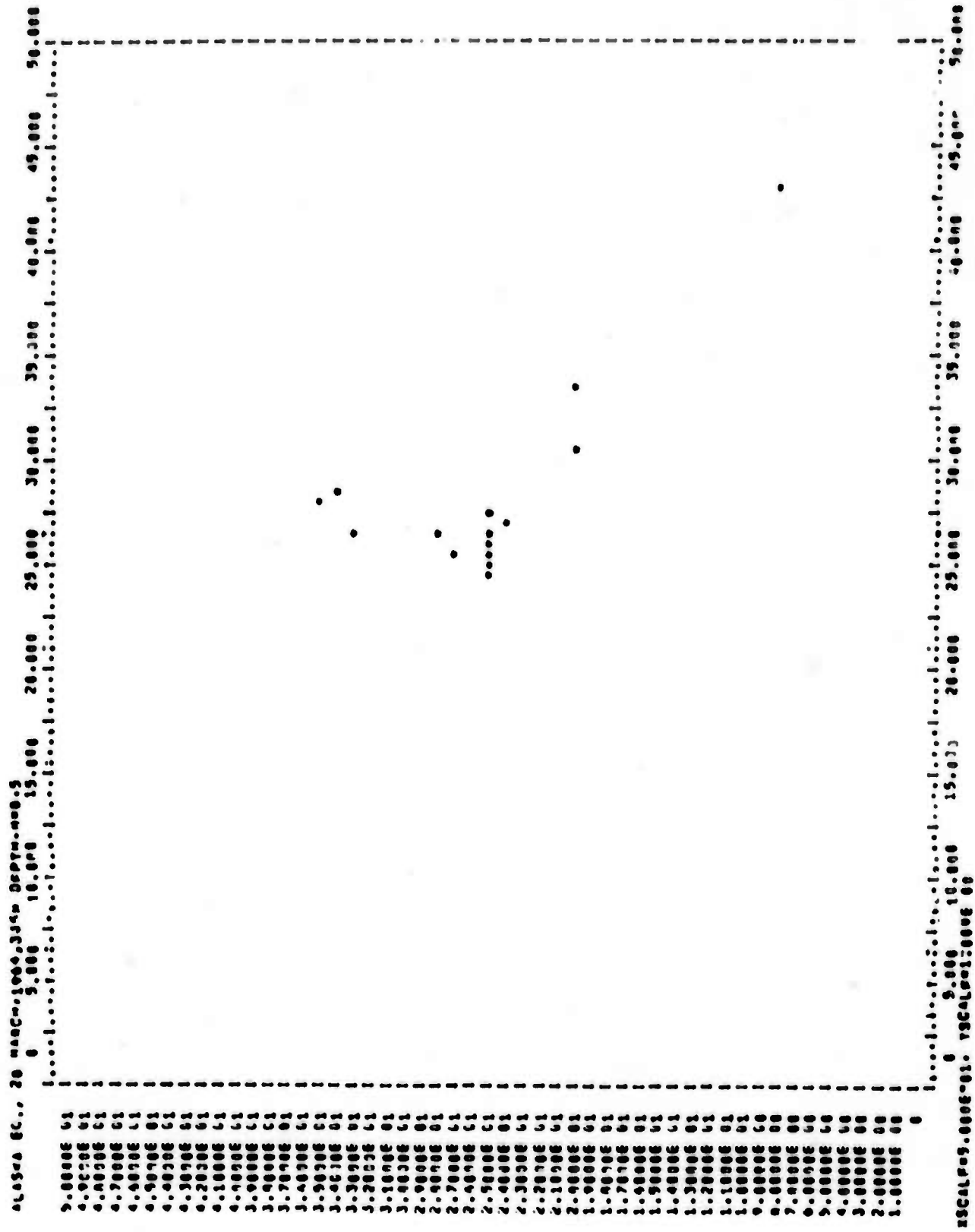


Figure 17. Observed Radiation Pattern for the Alaskan Earthquake of 28 March 1964.

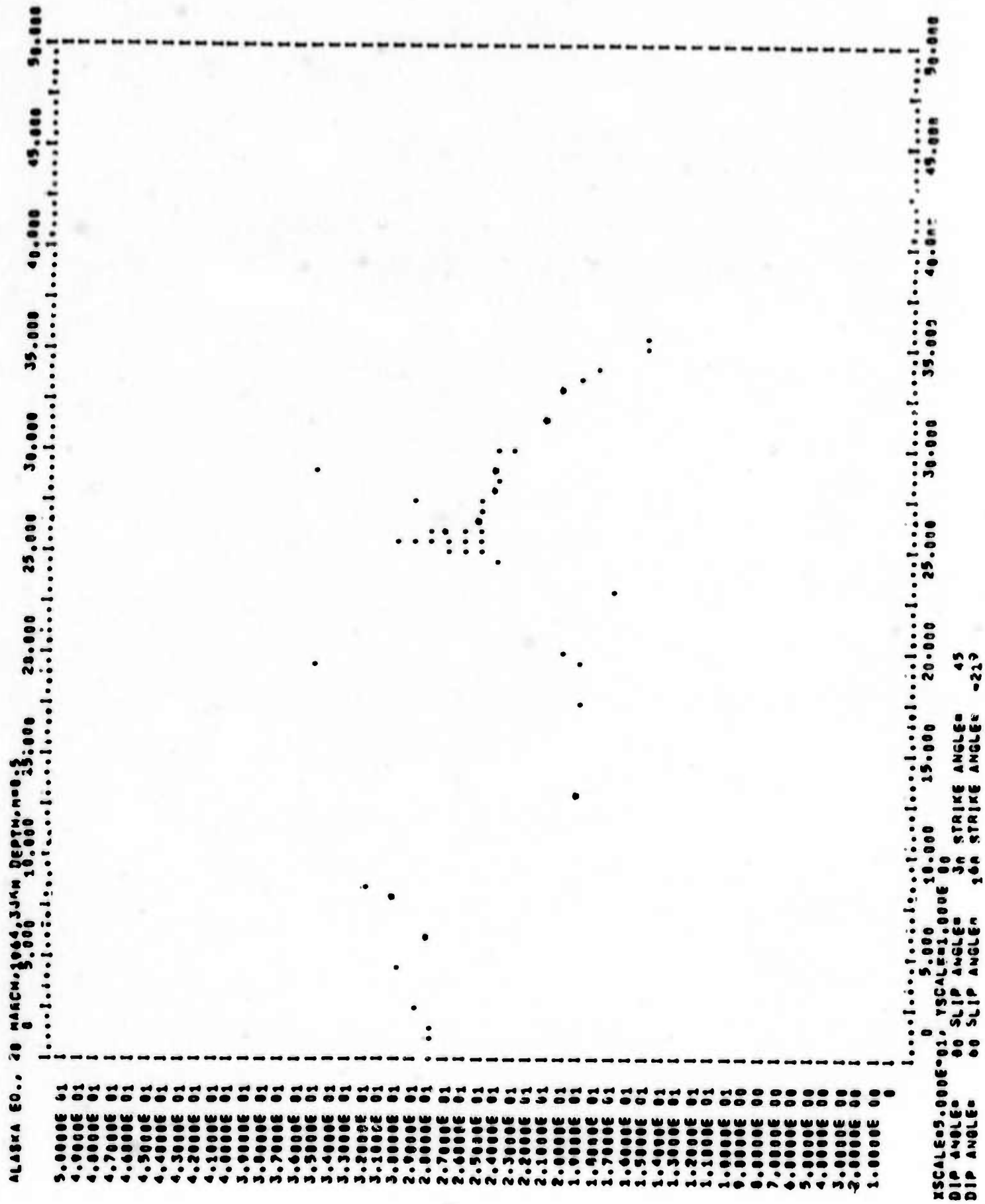
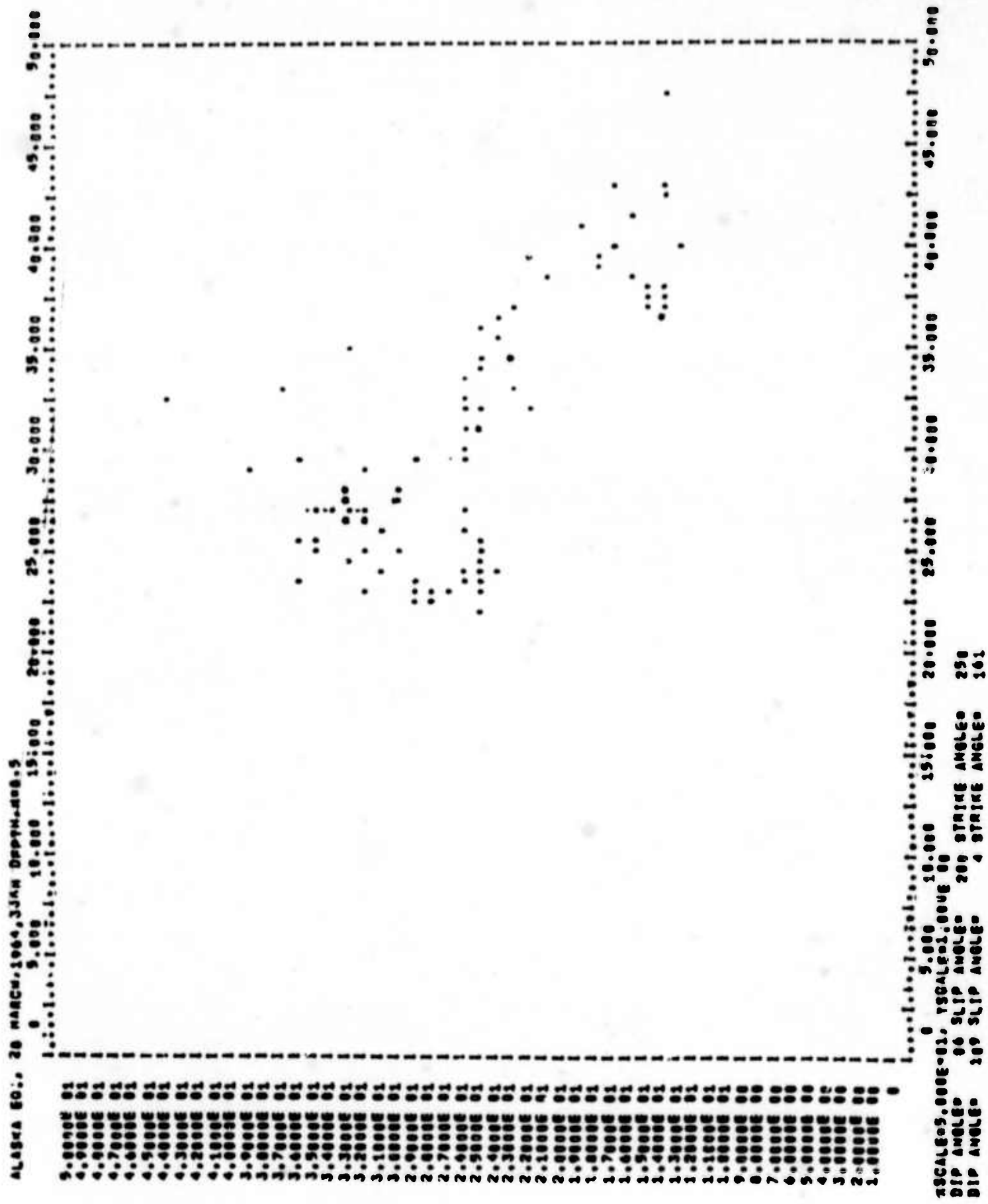


Figure 18. Calculated Radiation Pattern for the Alaskan Earthquake of 28 March 1964.





**Figure 19.** Calculated Radiation Pattern for the Alaskan Earthquake of 28 March 1964 (additional first motions).

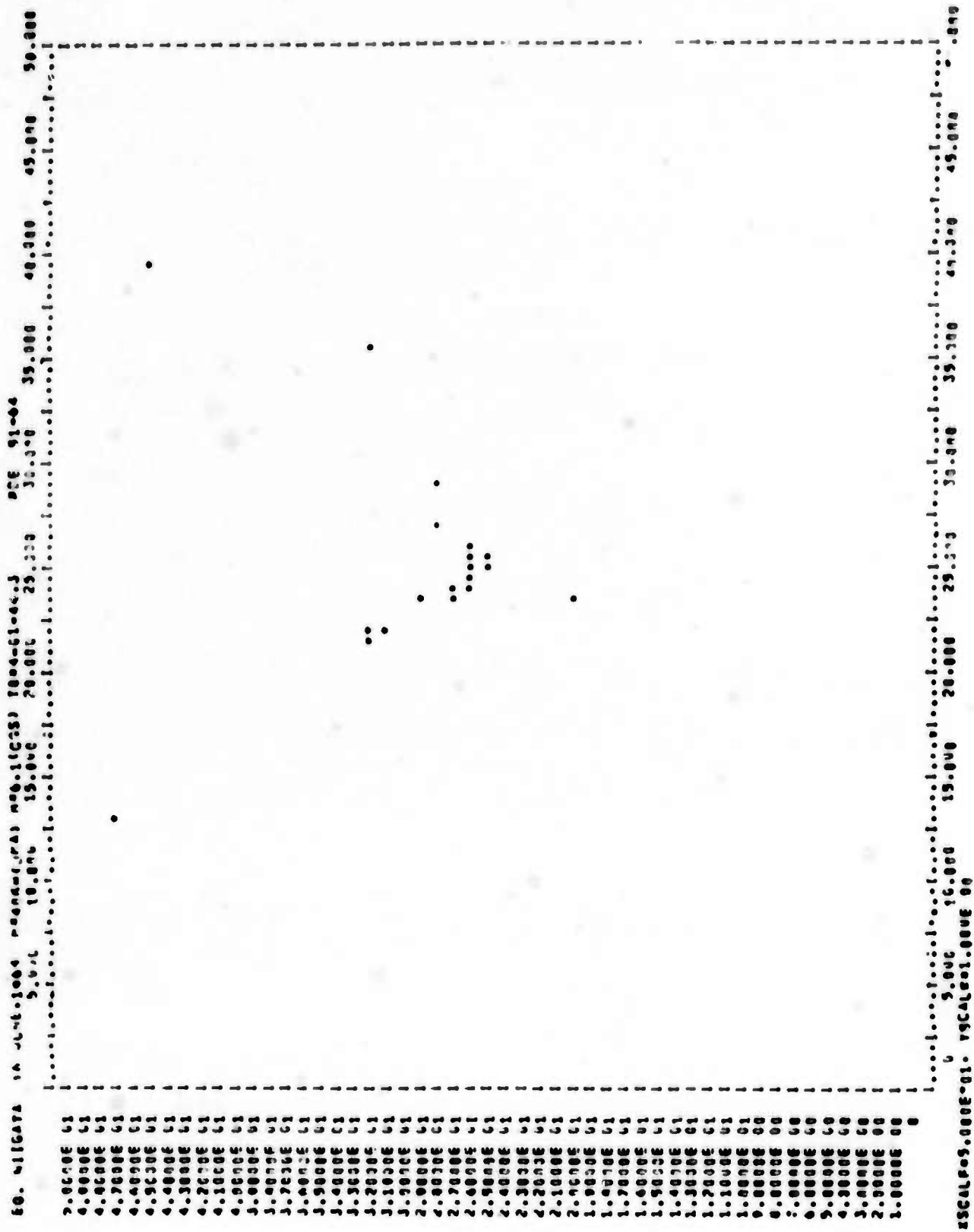


Figure 20. Observed Radiation Pattern for the Niigata Earthquake of 16 June 1964.

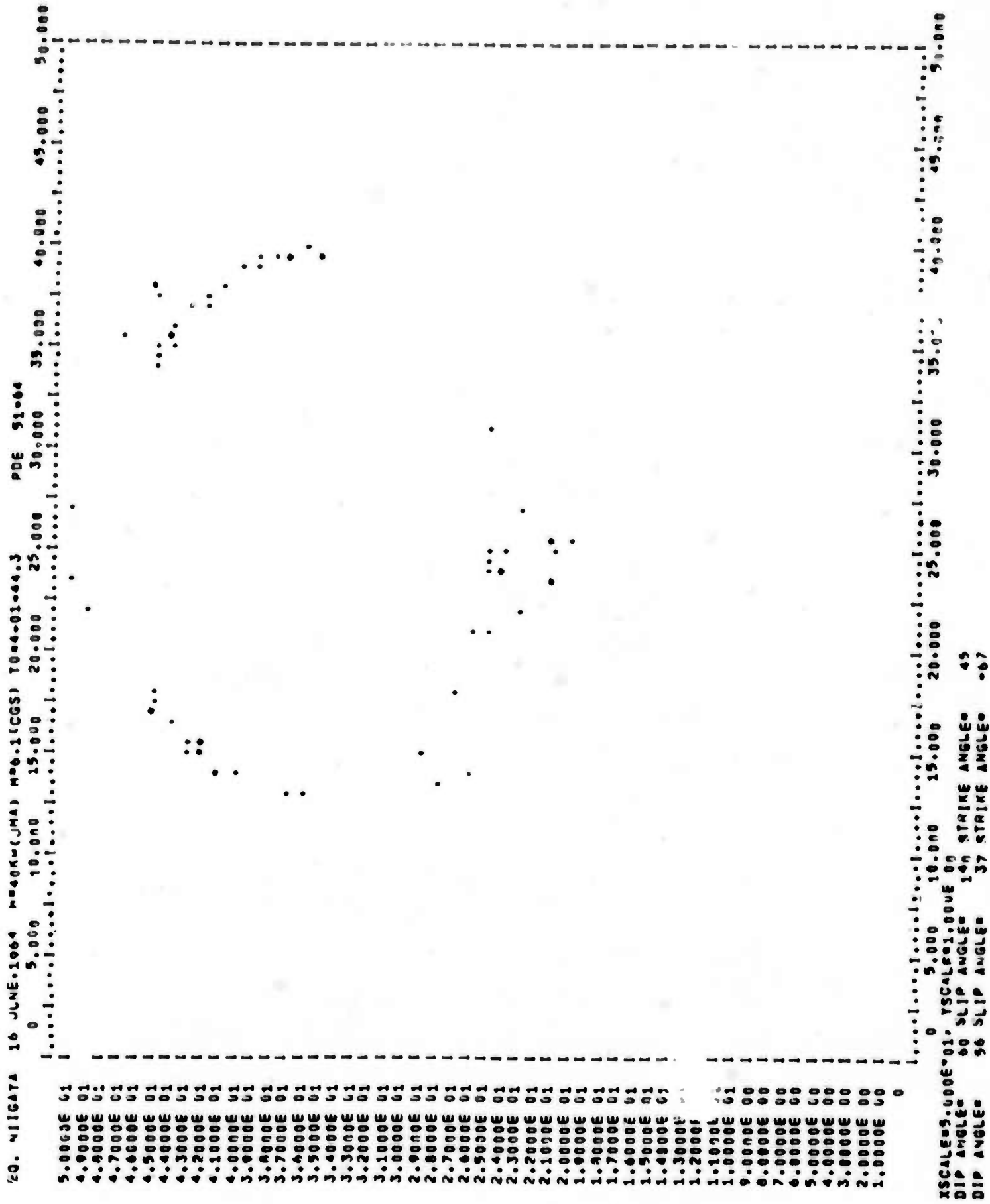


Figure 21. Calculated Radiation Pattern for the Niigata Earthquake of 16 June 1964.

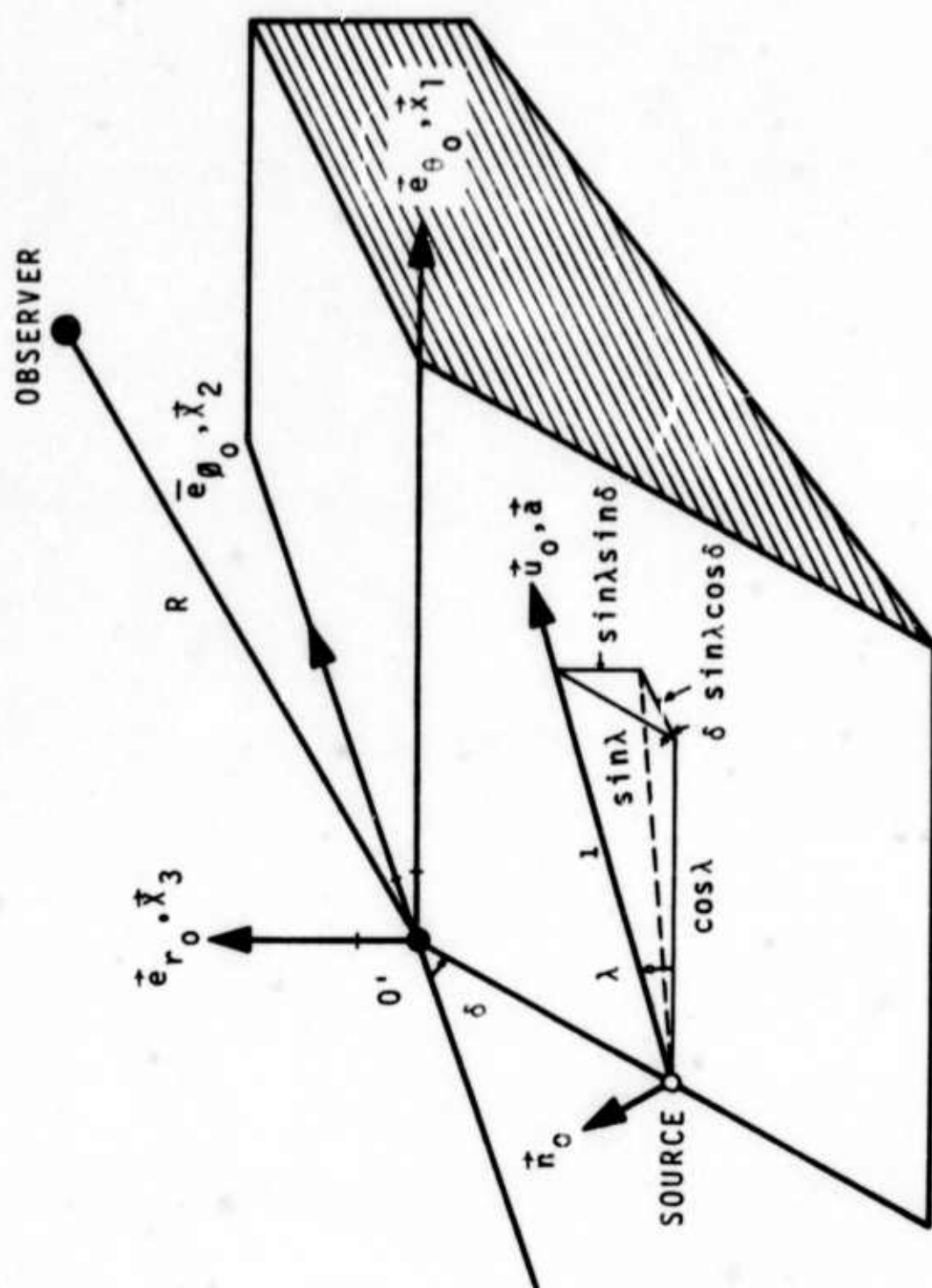


Figure 22. Geometry of a shear dislocation source

## APPENDIX

### Program RADPAT - Input Card Formats and Parameters

Part I (only read in once) Ritsema  $i - \Delta$  table.

1st card

NTAB	Col. 1-5	Number of values in table (I5)
------	----------	--------------------------------

2nd and subsequent NTAB/4 cards (8F10.2)

ANG(I)	Col. 1-10	$\Delta^\circ$ (F10.2)
--------	-----------	------------------------

X10(I)	11-20	$i_h^\circ$ (F10.2)
--------	-------	---------------------

Repeat for columns 21-40, 41-60, 61-80 as necessary

Part II (only read in once) - Gutenberg-Richter Distance-Depth

Correction Table (for use with input values of  $\log_{10} A/T$ ).

108 cards, each has format (4X, 17F4.1), hence every card contains 17 fields, for a depth of 0(25)100, 150(50)700 kilometers.

Part III - Earthquake data

1st card

N	Col. 1-5	Number of earthquakes to be treated (I5)
---	----------	--

2nd card

ID	Col. 1-80	Earthquake identification (10A8)
----	-----------	----------------------------------

3rd card

M	Col. 1-5	Number of stations (I5)
---	----------	-------------------------

ITAB	6-10	.LE.0 magnitudes are given as input (I5)
		.GT.0 $\log_{10} A/T$ is input and the
		Gutenberg-Richter correction is
		to be applied.



DEPTF 11-20 Depth of the hypocenter (F10.1)  
STRIKEO 21-30 Initial strike angle for the search (F10.1)  
DELSTRI 31-40 Increment in strike angle (F10.1)  
NSTRI 41-45 Number of increments to be used (I5)

Subsequent M cards contain the station data

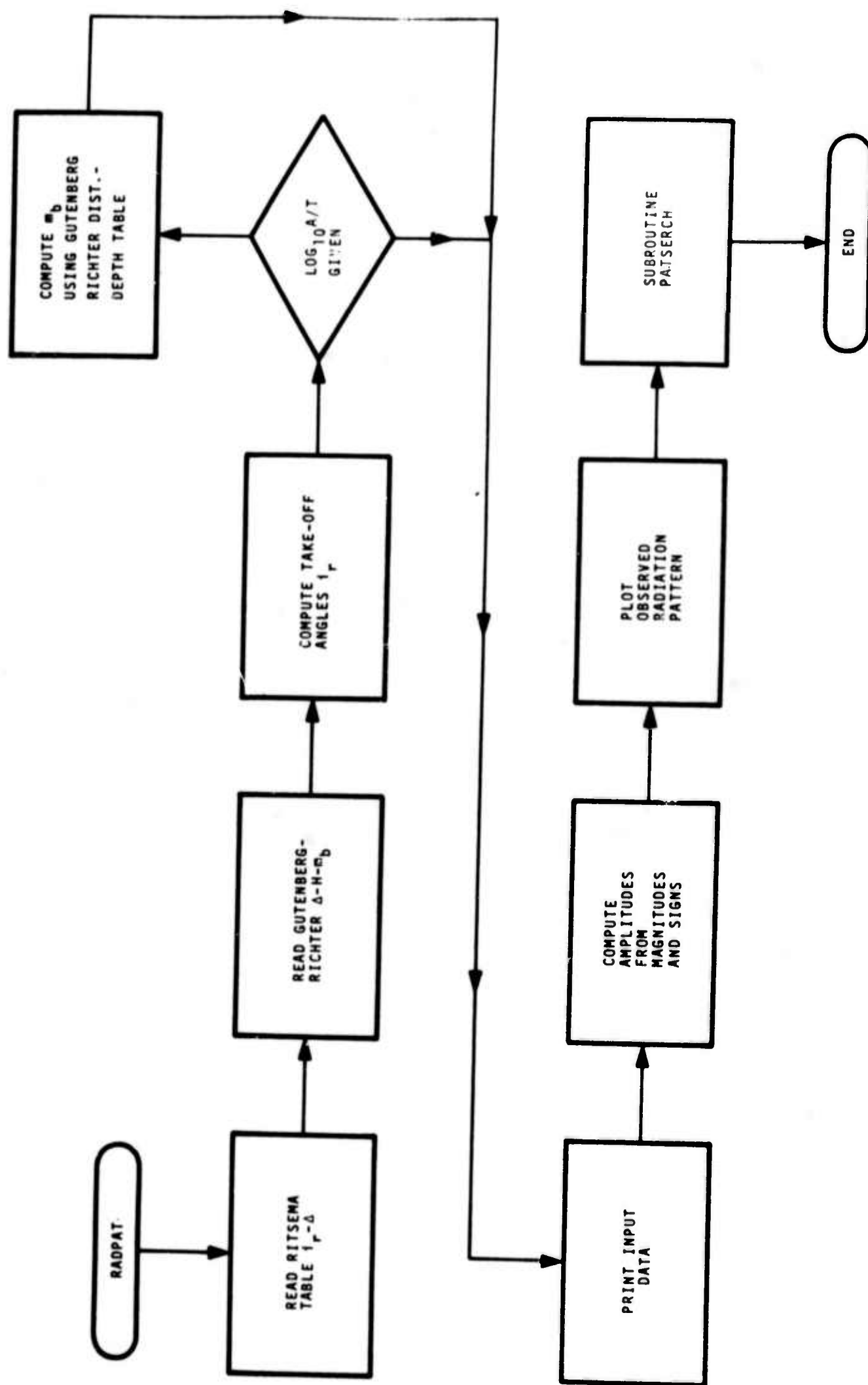
STA(I) 1-5 Station identification (A5)  
DIST(I) 11-20 Distance in degrees (F10.1)  
THETA(I) 21-30 Azimuth-epicenter-to-station in degrees (F10.1)  
MAG(I) 31-40 Magnitude or  $\log_{10} (A/T)$  (F10.1)  
ISIGN(I) 41-45 First motion direction (I5)

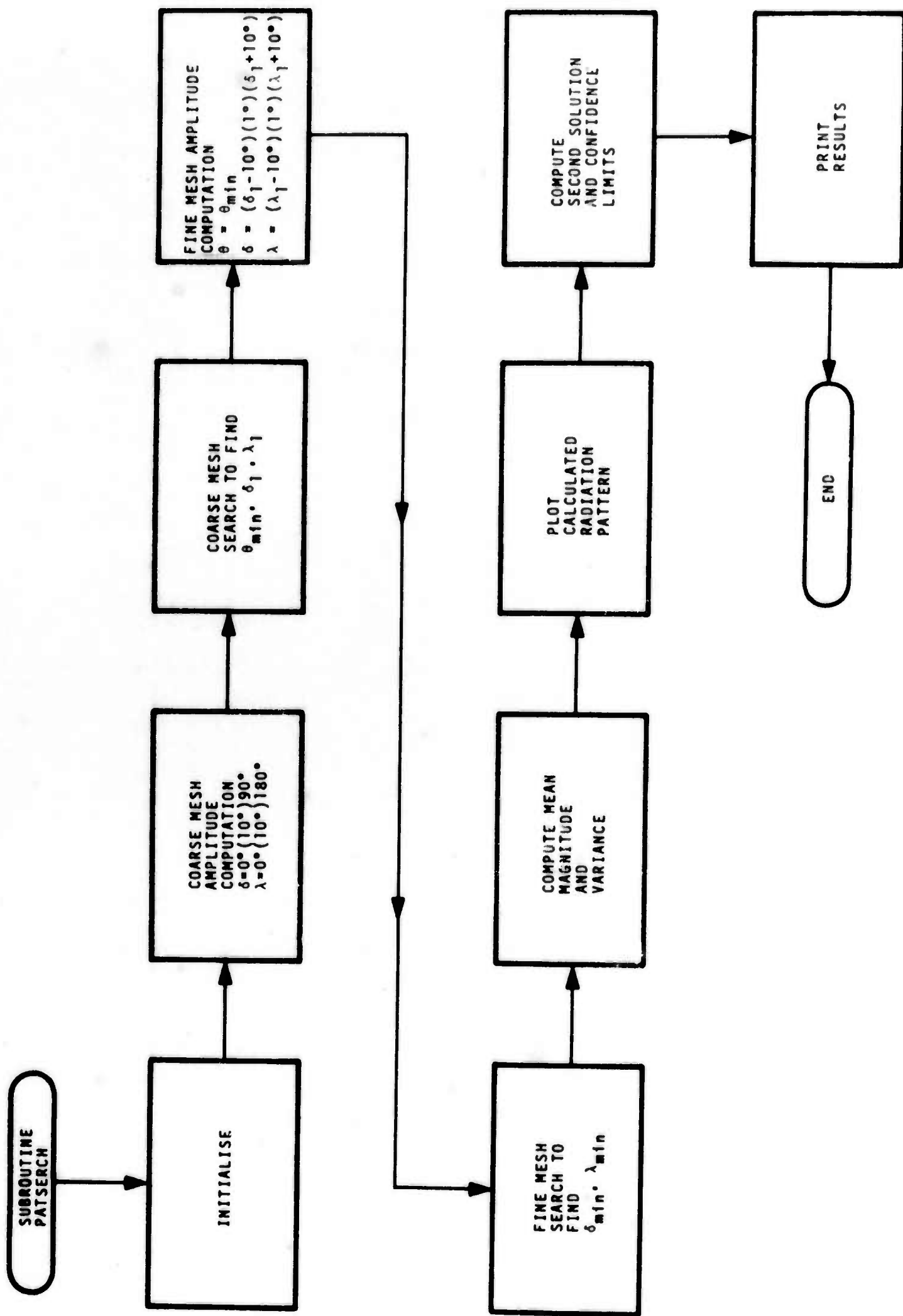
-1 indicates dilatation

1 indicates compression

0 or blank - if unknown, will be taken as  
compression







**Security Classification**

(Security classification of title, body of abstract and indexing annotation must be entered when the overall report is classified)

20. REPORT SECURITY CLASSIFICATION  
Unclassified

26 GROUP

## BODY WAVE MAGNITUDE AND SOURCE MECHANISM

## Scientific

Jarosch, H.S.,

30 September 1968

68

13

**F 33657-68-C-0945**

225

VELA T/6702

9b. OTHER REPORT NO(S) (Any other numbers that may be assigned to this report)

ARPA Order No. 624

ARPA Program Code No. 8F10

This document is subject to special export controls and each transmittal to foreign governments or foreign nationals may be made only with prior approval of Chief, AFTAC.

## 12. SPONSORING MILITARY ACTIVITY

ADVANCED RESEARCH PROJECTS AGENCY  
NUCLEAR TEST DETECTION OFFICE  
WASHINGTON, D. C.

A new method is proposed for improving the body-wave magnitude determination by using the observed values of the body-wave magnitude ( $m_b$ ) together with the first motion directions, to obtain by least squares analysis the best double couple source parameters; the resulting radiation pattern is then integrated spatially to provide a corrected estimate of the magnitude. Results for a number of events previously studied by other investigators are presented.

## Body Wave Magnitude

### Source Mechanism

**Security Classification**